Investigating the Impact of Chemotherapy Exposure on Peripheral Immune Responses for Patients with Ovarian Cancer

Investigating the Impact of Chemotherapy Exposure on Peripheral Immune Responses for Patients with Ovarian Cancer

Min Liu

A Thesis Submitted to the Faculty of

The Harvard Medical School

in Partial Fulfillment of the Requirements

for the Degree of Master of Medical Sciences in Immunology Harvard University

Boston, Massachusetts.

May, 2021

Thesis Advisor: Dr. Catherine J. Wu Min Liu

Investigating the Impact of Chemotherapy Exposure on Peripheral Immune Responses for Patients with Ovarian Cancer

Abstract

The current treatment of epithelial ovarian cancer (EOC) is based on surgical tumor debulking and platin-based chemotherapy. Neoadjuvant chemotherapy is used for initial tumor shrinkage before debulking surgery, but potentially also improves anti-tumor immune responses. Although the exact mechanisms are still unclear, we hypothesized that chemotherapy would lead to enhanced T cell responses.

To explore peripheral immune responses following chemotherapy, we tested the function of T cells from peripheral blood mononuclear cell (PBMC) samples over the course of chemotherapy using ELISPOT assays and evaluated the dynamics of T cell repertoire and immune cell composition changes using bulk and single-cell RNA sequencing.

T cells showed improved response to viral antigens after chemotherapy which was more pronounced in patients who initially responded to chemotherapy. Furthermore, we observed a trend towards increased central memory $CD8^+$ and regulatory T cells regardless of chemotherapy response, and higher T cell clonotype turnover in chemotherapy responders. Finally, chemotherapy led to increased frequencies of monocytes in peripheral blood with higher HLA class II expression. These findings are consistent with a model in which induction chemotherapy leads to disinhibition of T cell responses due to reduced tumor burden and decreased inhibitory signaling. This is additionally aided through increased antigen presentation by monocytes.

In sum, we provide evidence of immune-modulatory properties of chemotherapy in EOC which should be followed up in future studies.

Table of Contents

Figures

Acknowledgements

I would like to express my gratitude to my thesis advisor, Dr. Catherine Wu, for giving me the opportunity to work on this project and for the insightful feedback and guidance throughout my study. I am also very grateful to my mentors Dr. Derin Keskin, Dr. Panagiotis Konstantinopoulos, Dr. Livius Penter, and Dr. Guanglan Zhang for their help and guidance. I would like to acknowledge Dr. Shuqiang Li, Dr. Kenneth Livak, Dr. Nabihah Tayob for their assistance for this project.

I would also like to express my appreciation to Dr. Shiv Pillai, Dr. Michael Carroll, Dr. Gavin Porter, Selina Sarmiento, Faith Crisley, and all my classmates in the MMSc Immunology Program for their instruction, encouragement and camaraderie throughout the course of the program.

Finally, I must thank my parents and family for their support, accompany and concern all along the way.

"This work was conducted with support from Students in the Master of Medical Sciences in Immunology program of Harvard Medical School. The content is solely the responsibility of the authors and does not necessarily represent the official views of Harvard University and its affiliated academic health care centers."

Chapter 1: Background

Chemotherapy for cancer therapy

Cancer is one of the major public health issues in the world. It is also the second leading cause of death in the United States[1]. One of the earliest and primary treatments for cancer was chemotherapy. As early as the 1940s, aminopterin (later known as methotrexate) was used as the first chemotherapy drug that induced disease remission in children with acute lymphoblastic leukemia[2]. Nowadays, chemotherapy has become a systemic treatment that is widely used in hematologic malignancies and solid tumors. Although chemotherapy is often not curative for patients with advanced diseases, it has been shown to significantly improve progression-free survival[3]. Chemotherapy is often used in combination with additional treatment approaches such as radiation therapy or surgery. The administration of neoadjuvant chemotherapy is also important for improving surgical outcomes or can help to reduce disease burden prior to radiation or surgery for patients who are poor surgical candidates[2]. Different chemotherapy regimens are used based on the cancer types and the disease stages. Platinum-based chemotherapy (e.g., carboplatin) together with taxanes are common chemotherapy drugs for patient with EOC. Also, surveillance follow-up or maintenances therapy such as poly ADP-ribose polymerase inhibitors (PARPi)[4] and/or the VEGF-inhibitor Bevacizumab (BV)[5] are often provided as more targeted treatments after response to first line platinum-based chemotherapy for EOC patients.

Mechanisms of anti-tumor activity of platinum derivatives and taxanes

As a systemic cancer treatment, platinum analogs such as carboplatin eliminate cancer cells by inducing apoptosis or necrosis[6]. Specifically, carboplatin undergoes hydrolysis and becomes positively charged once it enters the cell membrane[7]. Positively charged carboplatin covalently

binds to the N7 site of purine bases and forms monoadducts or diadducts which disrupt cell replication[7]. Unlike platinum analogs, taxanes such as paclitaxel arrest the growth of cancer cells by stabilizing microtubules and lock dividing cells in metaphase on bipolar spindles by activating the spindle assembly checkpoint, which inhibits cell cycle progression[8]. Although the activity of commonly used chemotherapy drugs on highly replicative tumor cells is well understood, the mechanisms of chemotherapy that modulate endogenous host immune responses are still under investigation.

Ovarian cancer is a suitable model for studying the impact of chemotherapy on host immune responses

In order to investigate the mechanisms how chemotherapy impacts tumor immunity, an appropriate disease model is required. Epithelial ovarian cancer (EOC) is one of the major gynecological cancers with good prognosis when detected early. The estimated new cases and death of ovarian cancer in 2021 are 21,410 and 13,770[9]. However, the mild early symptoms of EOC often go unnoticed and explain why most patients with epithelial ovarian cancer are diagnosed at stage III or IV[10]. 5-year survival rates of stage III and IV ovarian cancer are 42% and 26%, respectively according to the report of ovarian cancer statistics in 2018[10]. The pathogenesis and origin of EOC have been revealed by recent morphologic, immunohistochemical, and molecular genetic studies[11]. According to the Cancer Genome Atlas, over 96% of advanced stage ovarian cancer patients harbor TP53 mutations[12]. Germline mutations of the BRCA1 and BRCA2 genes are found in 5–15% of women with ovarian cancer, and BRCA1/2 mutation has been shown as a high-risk factor for this disease[13].

One of the advantages of studying host immune responses to chemotherapy in EOC is the homogeneity of standard front-line regimens for its treatment. The standard of care treatments of EOC patients include neoadjuvant chemotherapy which aims to reduce the tumor size and primary surgical cytoreduction followed by standard chemotherapy regiments[14]. 63.5% of EOC patients with sage I and II and 79.9% patients with stage III and IV receive chemotherapy treatment[15]. Currently, the most common first-line chemotherapy drugs in treating EOC is the combination of platinum derivatives (e.g., carboplatin) with taxanes (e.g., paclitaxel), which is administrated for a total of 6 to 8 cycles for patients with advanced disease and 3 to 6 cycles for patients with the early stage EOC[16]. The combination chemotherapy drugs (e.g., paclitaxel-cisplatin) have led to improved clinical outcomes and survival rates of EOC patients[17]. A randomized trial of 680 advanced ovarian cancer patients has shown a beneficial outcome for patients on the paclitaxel-cisplatin regimen[18]. Patients with paclitaxel-cisplatin regimen had a 59% response rate, a median of 15.5 months of progression-free survival and 35.6 months of overall survival, which is 14% higher in complete clinical remission rates, 4 months longer in progression-free survival and 9.8 months longer in overall survival compared to standard cyclophosphamide-cisplatin regimen[18]. Clinical trials have also shown that there was no additional benefit for adding a third drug to the doublet chemotherapy[19].

Although platinum- and taxane-based chemotherapy is effective in treating primary ovarian cancer, over 70% of patients develop recurrence and chemoresistance[20]. Chemotherapy-induced bone marrow toxicity is known as the major cause of systemic immunosuppression. Common hematologic toxicities include leukopenia, anemia and thrombocytopenia, which are caused by RNA-protein crosslinking mediated suppression of hematopoietic cell growth and disruption of

cell proliferation[21]. Additionally, toxicities such as alopecia and neurotoxicity, are common problems for chemotherapy treatments[22]. In recent years, several clinical trials have tested semisynthetic docetaxel combined with carboplatin to reduce the toxicity of paclitaxel and other taxanes[23].

The availability of disease markers that can be monitored in peripheral blood is an advantage of EOC as a model tumor and provides the opportunity to evaluate host immunity in relationship to tumor burden. Cancer antigen 125 (CA125) is a 220- to 1000-kD tumor associated protein that is expressed by malignant cells such as fallopian tubes, endometrium, and peritoneum but not normal epithelial ovarian cells[24]. CA125 levels are elevated in 90% of advanced stage of EOC patients[25]. Accordingly, the reduction of CA125 level can be used an indicator of primary optimal surgical cytoreduction and long-term clinical outcome[26]. Studies have also shown a strong correlation between CA125 levels and chemotherapy response[27]. A rapid decline of CA125 value within 3 cycles of chemotherapy has been associated with superior outcome[27]. A study that evaluated CA125 values for at least 8 weeks following initiation of chemotherapy in 101 patients has shown that patients with a CA125 < 35 U/ml (n = 51) experience a median survival of 26 months compared to 15 months for patients with CA125 > 35 U/ml 8 weeks after initial chemotherapy treatment[28]. In addition, median survival of patients with serum CA125 value smaller and greater than 50% of their pre-treatment concentration were 21 months and 10 months, respectively[28].

Impact of chemotherapy on immune cells in the tumor microenvironment

The investigation of immunomodulatory effects of chemotherapy in the tumor microenvironment for EOC patients has been on-going in several groups[29,30]. Recent studies have demonstrated

multiple potential immune pathways that are differentially regulated following chemotherapy and several putative mechanisms of how chemotherapy modulates the host immune responses in the tumor microenvironment of ovarian cancer have been proposed. For example, paclitaxel can have immunostimulatory effects which promote anti-tumor immunity by upregulating the expression of MHC class I molecules or the presentation of tumor antigens[29] **(Figure 1A)**. Paclitaxel can also induce an immunoreactive tumor microenvironment by attenuating immunosuppressive regulatory T cells, promoting the expression of activation markers such as CD44 on $CD4^+$ and $CD8^+$ T cells, and increasing the production of IL-2 and IFN-γ in Th1 cells[31]. Moreover, the administration of docetaxel in tumor bearing mice reduced the number of myeloid-derived suppressor cells (MDSC) by sustaining the expression of alternative macrophage activation (M2) markers while promoting the classic activation macrophage (M1) markers in monocytes/macrophages in the tumor microenvironment[32] **(Figure 1B)**.

Unlike taxane drugs such as paclitaxel, platinum-based chemotherapy can modulate immunity in two directions. Evidence has suggested that tumor DNA damage triggered by platinum analogs could activate the STING pathway in antigen presenting cells and further increase T cell recruitment to the tumor microenvironment while promoting T cell exhaustion by upregulating PD-L1 expression[33]. Chemotherapy induced hematologic toxicities and upregulation of immune inhibitory molecules have driven the development of novel or combination therapy for ovarian cancer patients.

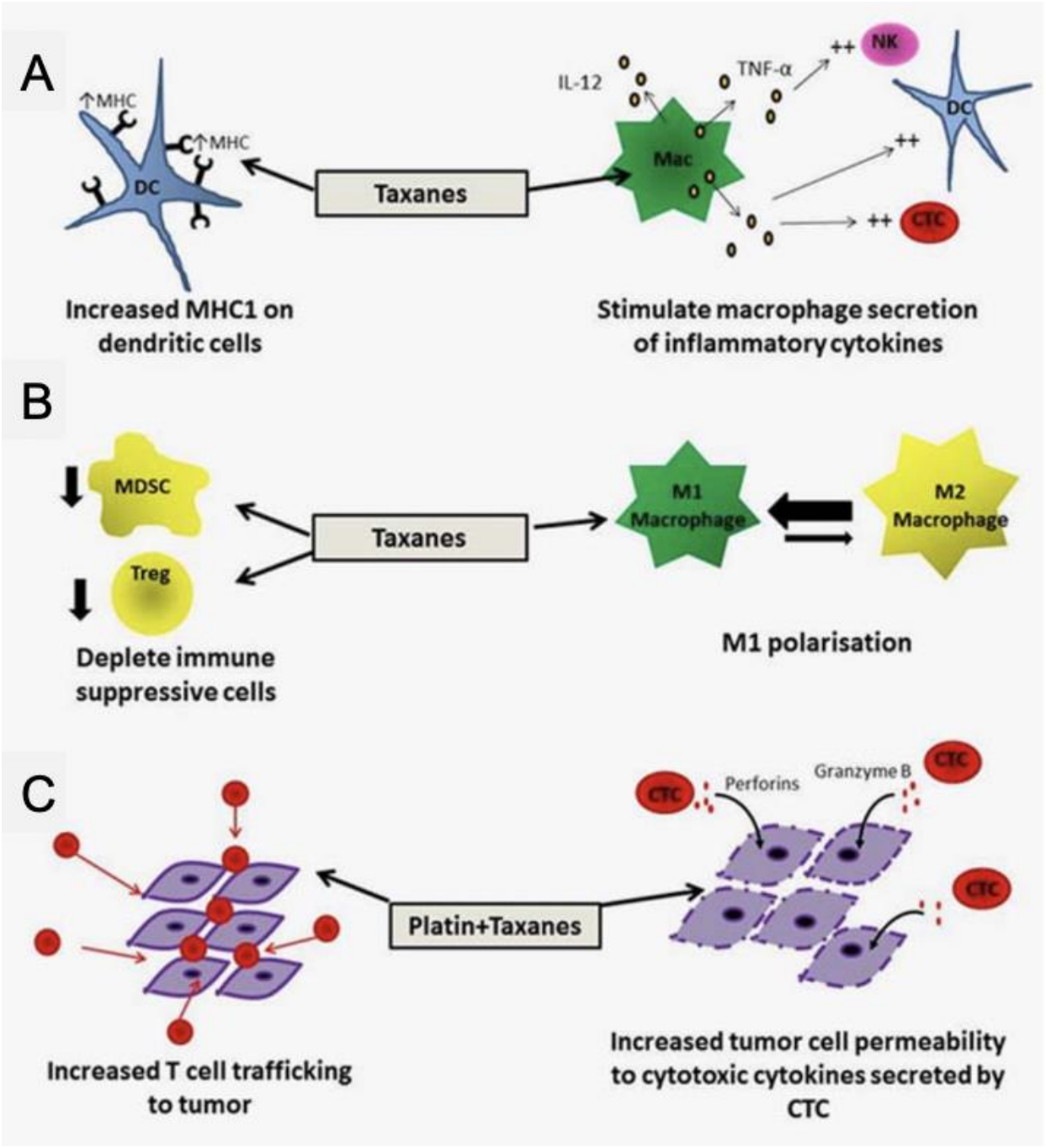

Figure 1. Immune modulatory effects of chemotherapy in the tumor microenvironment[34]
Chemotherapy drug such as carboplatin and taxanes can modulate host immune response through several mechanisms: **(A)** stimulating innate immunity by increasing the antigen presentation on dendritic cells and inducing the secretion of inflammatory cytokines in macrophages **(B)** alleviating the immune suppressive pressure by deleting myeloid derived suppressor cells or polarizing macrophages into pro-inflammatory phenotype **(C)** increasing T cell infiltration and enhance T cell toxicity.

Current efforts to develop combination therapies

Due to the non-specificity of chemotherapy and the high percentage of recurrence and chemoresistance in EOC patients, combination therapies are under investigation to improve remission rates and overcome chemoresistance. Several drugs have been tested in combination with chemotherapy. Dexamethasone is a glucocorticoid that is widely used as co-medication in treating solid malignancies to reduce the side effects of chemotherapy[35]. Intravenous administration of single-dose dexamethasone sodium phosphate (10 mg) immediately before chemotherapy reduced nausea and vomiting in patients receiving chemotherapeutic treatments[36]. Nevertheless, recent studies have indicated that dexamethasone significantly increased the adhesion of ovarian cancer cells to extracellular membrane and enhanced the apoptotic resistance of ovarian cancer cells to chemotherapy[37].

Poly [adenosine diphosphate (ADP) ribose] polymerase (PARP) inhibitors are being used as maintenance therapy for ovarian cancer patients in combination with surgery and chemotherapy[38]. PARP plays an important role in DNA damage-repair processes. PARP inhibitors such as niraparib and olaparib are known to directly cause cancer cell cytotoxicity through the propagation of DNA damage, indirectly stimulating dendritic cells and increasing T cell infiltration in the tumor microenvironment[39]. PARP inhibitors, however, can also upregulate the expression of programmed cell-death-ligand 1 (PD-L1) on tumor cells, which leads to immunosuppression[40]. Due to increased expression of PD-L1 induced by PARP inhibitors, clinical trials of antibodies inhibiting the immune checkpoint programmed cell death (PD-1) or its ligand (PD-L1) have been applied together with PARP inhibitors for treating EOC patients with acquired chemotherapy resistant or refractory disease[41]. The PARP and immune checkpoint inhibitor combination therapy

has shown a response rate of 18%, which exceeds the response rates of either PARP inhibitor or PD-1/PD-L1 blockade monotherapy[42]. However, the effectiveness of this combination therapy is still limited. Thus, novel combination therapies are urgently needed for EOC patients. In order to rationally design new combination immunotherapies, it is necessary to track and understand the dynamics of immune responses and immunomodulatory effects of chemotherapy on immune cells over the course of chemotherapy.

Monitoring host immune responses to chemotherapy in peripheral blood

The immune landscape is a key predictor for clinical benefit from cancer treatments and a better understanding of the host immune status could help to predict responses to the treatment. Although tumor samples are commonly used for studying immune responses and tumor microenvironment, serial sampling is often either not possible[43] or comes at high risks for the patient[44]. During the past decade, researchers have been analyzing circulating biomarkers using peripheral blood samples for cancer prognosis which allows for repeated measurements. Analyzing readily accessible peripheral blood samples could also be an effective way to monitor host immune responses. Multiple peripheral leukocyte subpopulations have shown to be associated with responses to cancer therapy[45]. For example, increases of effector cell populations from baseline to on-treatment timepoints have been shown to correlate with positive treatment outcomes, while poorer outcomes are often associated with high frequencies of inhibitory subpopulations such as regulatory T cells and myeloid-derived suppressor cells[46].

Advanced techniques in studying the host immune responses

The development of techniques and accessibility to massively parallel sequencing has opened new chapter for biological and medical research. One of the major achievements has been the automated digital sensors for data collection in a large volume. A premier example is the improvement of the high-throughput sequencing techniques. Originated in the 1970s, the initial sequencing protocols were highly laborious and inefficient[47]. The pace of sequencing has dramatically accelerated with the invention of automated digital instruments in the past 20 years[48]. A growing number of technologies were invented to measure the average response of a heterogeneous population of cells, or bulk measurements[49]. These tools facilitate the generation of highly multiplexed data and analyses, which are important for monitoring the immune system such as profiling of treatment-induced T cells multidimensionally and longitudinally[49]. Nonetheless, the averaging of parameters in bulk measurements makes the detection of rare cell types, specific phenotypic states of the cells, co-regulation of genes and causality of events challenging[50]. To enable identification of transcriptome changes and cellular subtypes in immunological responses, single cell technologies have been developed for both depth and breadth of measurements. Recent advanced microfluidic technologies such as the 10x Chromium Controller instrument (10x Genomics) are able to analyze hundreds to tens of thousands of single cells in each run in a more cost-effective manner[51]. This high-throughput single cell profiling makes it possible to uncover the gene expression variability in each cell and identify rare cell types in heterogenous samples[52]. Furthermore, paired full-length T cell receptor (TCR)/ B cell receptor (BCR) sequencing and CITE-seq allows researchers to analyze surface protein expression, gene expression, and antigen specificity at the single cell level[53]. However, the great quantities of data generated by the instruments require advanced bioinformatics pipelines for analysis.

Consequently, the second important advance in the field has been the development of computational and analytical tools in processing the data. These approaches include advanced search and indexing algorithms, large-scale high-performance processing systems, sequence-pair modeling through deep learning, statistical inference for expression quantification, and many more[54]. For example, in single cell RNA sequencing, splice-aware alignment (STAR) and pseudo-alignment (kallisto) methods are developed to reduce the noise in BWA transcriptome mapping strategy[55]. In addition, differential expressed genes are detected by empirical Bayes methods such as edgeR to estimate gene-specific biological variation[56]. In order to visualize the high-dimensional gene expression in a more informative manner, dimensionality reduction strategies such as principal component analysis (PCA), independent component analysis (ICA) and various non-linear methods such as t-distributed stochastic neighbor embedding (t-SNE) are widely used in visualizing the cell clusters[57]. The advanced sequencing and analytical tools have greatly improved the efficiency and accuracy of the data generation and interpretation.

Chapter 2: Data and Methods

Overview

Chemotherapy aims to reduce tumor size before cytoreduction or destroy the remaining tumor cells after debulking surgery. However, chemotherapy not only kills highly dividing tumor cells but can also eliminate immune cells. Therefore, our goal was to understand the changes in immune status and composition of circulating immune cells following chemotherapy. Ten patients with stage IIIC or IV epithelial ovarian cancer received standard of care platinum-based chemotherapy at the Dana-Farber Cancer Institute **(Figure 2A)**. 8 of 10 patients in this study received 6 cycles of chemotherapy with primary tumor cytoreductions between the third and sixth cycles of chemotherapy **(Figure 2A)**. Among the rest of the 2 patients, one received 5 cycles of chemotherapy while the other received 7 cycles of chemotherapy and no primary tumor cytoreduction **(Figure 2A)**. In addition, all patients received 20 mg dexamethasone every 3 weeks for all 6 cycles of chemotherapy **(Figure 2A)**. Neupogen and/or Neulasta, different forms of filgrastim (recombinant granulocyte colony-stimulating factor [G-CSF]), were administrated in 8 out of 10 patients with various dosing schedule to reduce chemotherapy-induced neutropenia **(Figure 2A)**. To investigate the impact of chemotherapy exposure on the peripheral immune responses in ovarian cancer patients, blood samples were collected from 10 patients at pre-chemotherapy (Baseline), third cycle (C3), sixth (C6) cycle of chemotherapy, and 1–2-month post chemotherapy (Post) **(Figure 2B)**. To monitor the degree of the tumor and the efficacy of chemotherapy, cancer antigen 125 (CA125) levels of all 10 patients were tested **(Figure 2C)**. Clinical Complete Blood Count (CBC) values were also measured to track the number of blood neutrophils, monocytes, and lymphocytes throughout chemotherapy **(Figure 2D)**. To perform the downstream analyses of patients' immune responses to chemotherapy, peripheral blood

mononuclear cells (PBMCs) at Baseline, C3, C6, and Post of the 10 patients were isolated from blood samples using Ficoll density gradient centrifugation (GE healthcare). IFN-γ ELISPOT responses were measured on 7 patients to test the peripheral T cell functions against OVA (negative control), FluA, and CEF peptide pool (viral epitopes from viral epitopes from Cytomegalovirus, Epstein-Barr virus, and Influenza) at each stage (Baseline, C3, C6, and Post) of chemotherapy **(Figure 3)**. After examining the functions of T cells over the course of chemotherapy against common viral antigens, bulk TCR sequencing adapted RNase H-dependent TCR-sequencing (or bulk TCR sequencing) [58] was performed on the T cells isolated from PBMCs from 8 patients to investigate the dynamics of the peripheral T cell repertoire following chemotherapy **(Figure 4)**. Furthermore, single-cell RNA sequencing was performed on 5 patients at pre-chemotherapy and after the third cycle of chemotherapy to identify the immune cell compositions of the patients and exam the dynamics of immune cells after chemotherapy **(Figure 5 and Figure 6)**. Finally, to link changes in T cell clonality with T cell phenotypes after chemotherapy, single-cell RNA and TCR sequencing were performed on 5 patients at pre and third cycle after chemotherapy **(Figure 7 and Figure 8)**.

Materials and Methods

Patient PBMC samples

Heparinized blood samples were obtained from 10 patients at Dana-Farber Cancer Institute and stored in vapor-phase liquid nitrogen until time of analysis. Serum CA125 concentrations of the patients were measured using electrochemiluminescence immunoassay[59]. Complete blood count, including red blood cell count, white blood cell count, platelet count, absolute lymphocyte counts, absolute monocyte counts, absolute neutrophil counts were measured by Gynecologic CRIS Team

at Dana-Farber Cancer Institute. Ficoll density gradient centrifugation (GE healthcare) was performed to isolate patient PBMCs. Isolated PBMC samples were cryopreserved with 10% DMSO in FBS (Sigma-Aldrich).

IFN-γ ELISPOT assay

To pre-stimulate T cells in vitro, 24-well culture plates were used for PBMCs stimulation with individual (FluA or OVA) or each pooled peptide (CEF) and incubated overnight. Normalized results were presented by spot forming cell (SFC) per 1×10^6 cells. T cell specificity and functionality were tested against FluA, CEF peptide pool (viral epitopes from viral epitopes from Cytomegalovirus, Epstein-Barr virus, and Influenza), and OVA peptide by IFN-γ ELISPOT in DMEM medium supplemented with 5% penicillin–streptomycin, 10% FBS, HEPES, β-mercaptoethanol, sodium pyruvate, and nonessential amino acids. Positive responses were scored if > 55 spot-forming cells and at least 3 standard deviations over the OVA control were detected. In the ELISPOT analysis, an average of the control (OVA) for each time point was calculated and data for each antigen peptide (FluA or CEF) were normalized against the control by subtracting the average of the control from each of the three replicate pool measurements at the corresponding time. Zero was substituted if the normalized value was smaller than zero. *P*-value was calculated using the repeated-measures mixed-effect model and corrected for multiple comparisons with Dunnett's test. Relative spot forming cell (SFC) at each time point after chemotherapy compared to Baseline was calculated based on the SFC before background removal. Values below 3-standard deviation of OVA control were replaced by the 3-standard deviation of OVA control.

RNA extraction

Prior to RNA extraction, cryopreserved PBMCs collected from patients were thawed in DMEM complete medium. AB-positive heat-inactivated human serum (Gemini Bioproduct), 10% FBS, HEPES, sodium pyruvate, 5% penicillin–streptomycin, β-mercaptoethanol, and nonessential amino acids were used as supplement. RNA was collected from 5×10^6 PBMCs using the RNeasy Mini Kit (Qiagen).

Bulk TCR sequencing and analysis

The adapted RNase H-dependent TCR-sequencing protocol was performed on bulk RNA samples for α and β TCR repertoire analysis[58]. Four to eight replicates were performed for each bulk RNA sample after reverse transcriptase reaction. Exonuclease digestion was performed to eliminate excess reverse transcriptase primers before running RNase H-dependent PCR. After sequencing library generation, bulk RNA samples were sequenced using the MiSeq 300 cycle reagent kit v.2 on the Illumina sequencing platform according to the manufacturer's protocol[60]. The sequencing data analysis was performed using R. A Fisher's exact test with correction for multiple hypothesis testing (Benjamini-Hochberg FDR procedure) was performed to detect T cell clonotypes with statistically significant changes in frequency. T cell diversity was calculated using a Shannon Index[61]. To reduce the variation causes by sequencing depth, we normalized the Shannon index through division by the natural log of total number of reads in each sample. T cell clonotypes were annotated by matching the CDR3 amino acid sequences of the T cell α or β chains of each patient to the corresponding CDR3 amino acid sequences of T cell α or β chains in the VDJdb[62] and MCPAS-TCR[63] databases.

Single cell RNA sequencing analysis

The samples processed for single cell RNA sequencing were obtained from the PBMC samples isolated after Ficoll density gradient centrifugation. Dead cells were removed from PBMC samples using a dead cell removal kit (Miltenyi Biotec). The viable cells were washed and resuspended in PBS with 0.04% BSA at a cell concentration of 1000 cells/µL. 17,000 viable cells were loaded onto a 10× Genomics ChromiumTM instrument (10x Genomics) according to the manufacturer's recommendations. The single cell RNA sequencing libraries of patients 4, 9, and 13 were processed using the Chromium Next GEM Single Cell 5' Kit v2 (10x Genomics). The single cell RNA sequencing libraries of patients 2 and 3 were processed using the Chromium Single Cell 5' Library & Gel Bead Kit (10x Genomics). Matched single cell TCR libraries were prepared using the Chromium Single Cell Human TCR Amplification Kit (10x Genomics). Quality controls for amplified cDNA libraries, TCR sequencing libraries, and final sequencing libraries were performed using the Bioanalyzer High Sensitivity DNA Kit (Agilent). The sequencing libraries for single cell RNA sequencing and single cell TCR sequencing were normalized to 4nM concentration and pooled using a volume ratio of 4:1. The pooled sequencing libraries of patients 4, 9, and 13 were sequenced on the Illumina NovaSeq S4 300 cycle platform (sequencing parameters: Read 1 of 150bp, Read 2 of 150bp and Index 1 of 8bp) and for patients 2 and 3 on the NovaSeq SP sequencing platform (sequencing parameters: Read 1: 26nt, Read 2: 91nt, Index 1: 8nt). The sequencing data were demultiplexed and aligned to GRCh38 using the cell ranger version 5.0.0 pipeline (10x Genomics). Cells from all time points and all patients were combined. Quality control (QC) was performed to exclude cells with (1) fewer than 500 or more than 15000 UMIs; (2) fewer than 300 genes; (3) fewer than 0.8 UMIs per gene; and (4) mitochondrial ratio <0.2 (number of UMIs assigned to mitochondrial genes over total number of UMIs per cell). 3.26% of

cells were excluded after QC. All the cells passing QC were integrated and clustered using Seurat v3[64]. Differential expressed (DE) analysis was performed between time points (Base and C3) and clusters using the default Wilcoxon rank-sum test implementation in Seurat. DE analysis was performed on the patient combined dataset and on each patient to avoid bias in DE calling. Although variations of DE genes in monocytes among patients after chemotherapy were observed, the upregulated genes at C3 in the combined patient dataset reflected the overall transcriptional changes of all the patients (Extended Data Figure 4A). T cell states were predicted using Seurat reference datasets which applied unsupervised 'weighted-nearest neighbor' (WNN) analysis and incorporate RNA sequencing and CITE sequencing of 211,000 human PBMCs, with large cell-surface protein marker panels[65]. Single cell datasets of healthy donor PBMCs were downloaded from the 10X Genomics (5k PBMCs from a healthy donor (v3 chemistry) and PBMCs from a Healthy Donor: Whole Transcriptome Analysis) and Seurat [65].

Results

Monitoring residual tumor burden in ovarian cancer patients following chemotherapy

To track the tumor size and the effectiveness of chemotherapy for ovarian cancer patients involved in this study, CA125 levels were measured before, during, and at after 2 months of chemotherapy with CA125 blood test. We observed that CA125 levels of all 10 patients declined dramatically after chemotherapy treatment **(Figure 2C)**. Patient 5, 7, 8, 9, 10 experienced rebounds of CA125 levels at post chemotherapy follow-up, which indicated potential relapses after chemotherapy **(Figure 2C)**. Interpretation of serum CA125 level has been based on the normal CA125 level derived by screening the blood from healthy women of reproductive ages[66]. In this study, chemotherapy non-responders referred to patients whose CA125 levels did not normalize to 38 U/ml or lower after the third cycle of chemotherapy and remain higher than 100 U/ml before interval debulking surgery. Based on the criteria of chemotherapy response as described above, patients 2, 3, 9, 10, 12, and 13 were chemotherapy responders while patients 4, 5, 7, and 8 were chemotherapy non-responders **(Figure 2C)**.

Tracking the changes of blood cells after chemotherapy

To access the impact of chemotherapy on blood cells, clinical CBC values were measured to track the blood cells including monocytes, neutrophils and lymphocytes over the course of chemotherapy. Statistically significant increases of absolute monocyte and lymphocyte counts were detected after chemotherapy **(Figure 2D)**. In contrast, absolute neutrophil counts were decreased **(Figure 2D)**. Neupogen and Neulasta are commonly injected during chemotherapy to stimulates the growth of neutrophils. The administration of Neupogen and/or Neulasta, however, was not associated with neutrophil counts in our patients (data not shown). Nevertheless, the

neutrophil to lymphocyte ratio has been shown to associate with the chemotherapy response and patients' outcome. Studies have indicated that patients with increased neutrophil-to-lymphocyte ratio were at a higher risk of disease progression[67]. In our study, the median neutrophil-to-lymphocyte ratio of the patients decreased over time throughout chemotherapy, which indicates a potential recovery of immune responses after chemotherapy **(Figure 2E)**. The decreased CA125 levels and neutrophil-to-lymphocyte ratio in the patient cohort suggested that chemotherapy reduced the tumor size and could potentially alleviate the inhibition of immune responses exerted by the tumor.

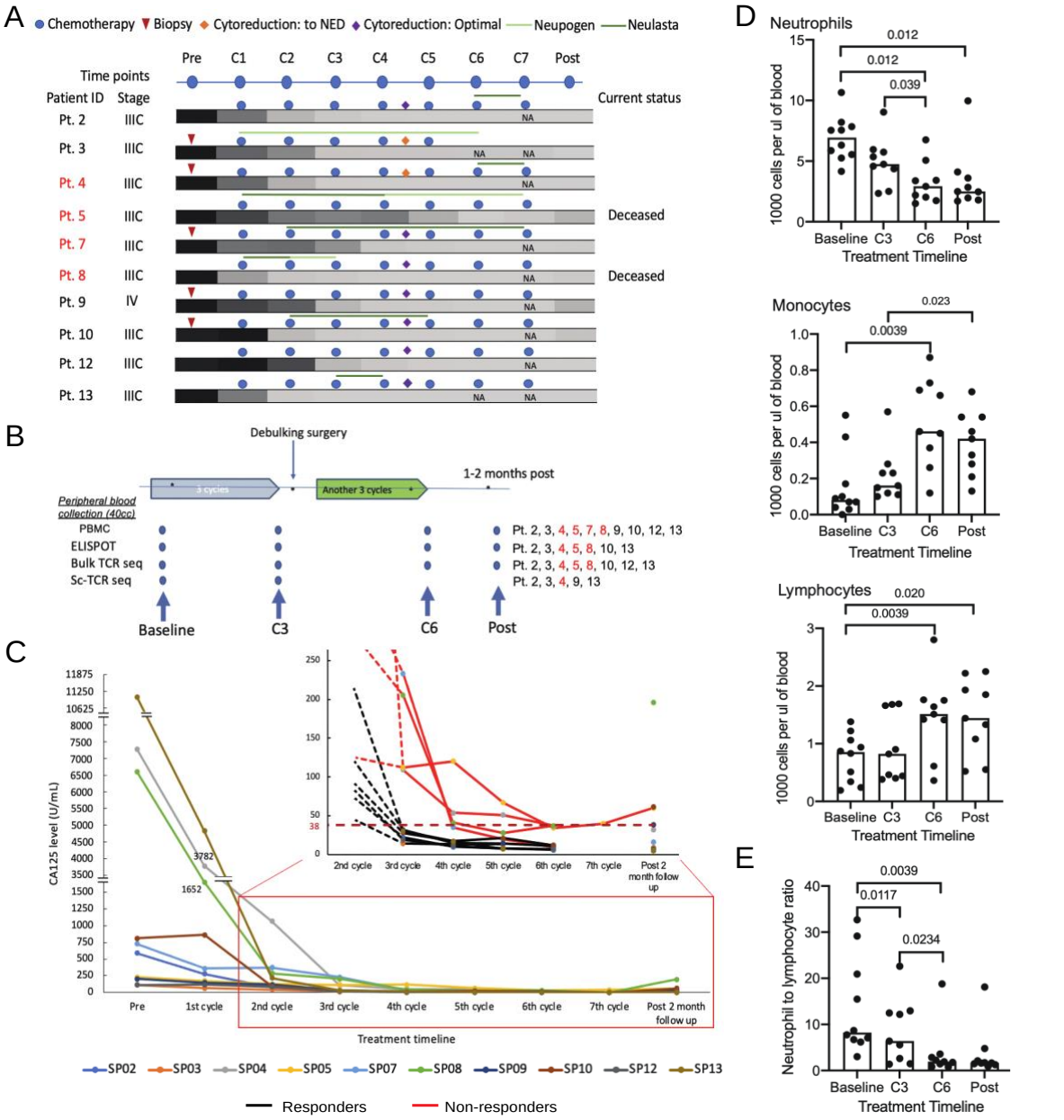

Figure 2. Overview cohort and clinical information

(A) Treatment schedule for the ten ovarian cancer patients who received at least five cycles of chemotherapy. Grey bars - relative CA125 level for each individual patient. Patients labeled in red are chemo non-responders. **(B)** Experimental schema of the study. PBMCs were collected at Baseline, C3, C6 and Post chemotherapy from 10 patients. ELISPOT assay was performed at Baseline, C3, C6 and Post chemotherapy on 7 patient samples. Bulk TCR sequencing of 8 patient samples at Baseline, C3, C6 and Post chemotherapy were performed and analyzed. Baseline and C3 samples of 3 patients were used for single cell RNA sequencing. Patients labeled in red are chemo non-responders. **(C)** Absolute CA125 levels for each individual patient. **(D, E)** Absolute CBC values (C) and neutrophil to lymphocyte ratio (D). Each bar represents the median CBC value of each patient cohort. Statistical testing using Wilcoxon rank sum test.

Improved peripheral T cell function following chemotherapy

T cells play an important role in antitumor immunity. Cytotoxic T cells, for example, can recognize tumors or viral antigens after priming by antigen presenting cells. Nevertheless, there is evidence that chemotherapy not only eliminates tumor cells but can also impede T cell functions by upregulating PD-1 expression, which may further reduce the T cell mediated antitumor or antiviral immunity in patients[30]. A long-term follow-up study in breast cancer patient, however, demonstrated restoration of T cell responsiveness after chemotherapy and radiation therapy[68]. To test whether chemotherapy inhibited the overall T cell function of our patients, we used ELISPOT assays to evaluate the T cell responses against common viral antigens in 7 patients. T cell responses against FluA or CEF antigen were detected by IFN-γ ELISPOT assay in all 7 patients. Chemo responders (Patient 2, 3, 10, and 13) exhibited increases in T cell responses to either FluA or CEF peptide pool **(Figure 3A and Extended Data Figure 1A)**. Chemo non-responders (Patient 4, 5, and 8), also exhibited increases of T cell response to FluA or CEF during chemotherapy treatment **(Figure 3B and Extended Data Figure 1B)** but were delayed compared to responding patients. The relative changes of spot forming cells over the course of chemotherapy also indicated a trend of higher and faster T cell responses to viral antigens in chemo responders **(Figure 3C)**. Overall, the data suggested that T cell functions were recovered in response to viral antigens in both chemo responders and non-responders after chemotherapy. With respect to the more rapid decrease of CA125 levels and increase of T cell responses in chemo responders, we interpret the greater reduction of tumor burden in chemo responders to result in a less immunosuppressive environment and thus faster recovery of T cell responses.

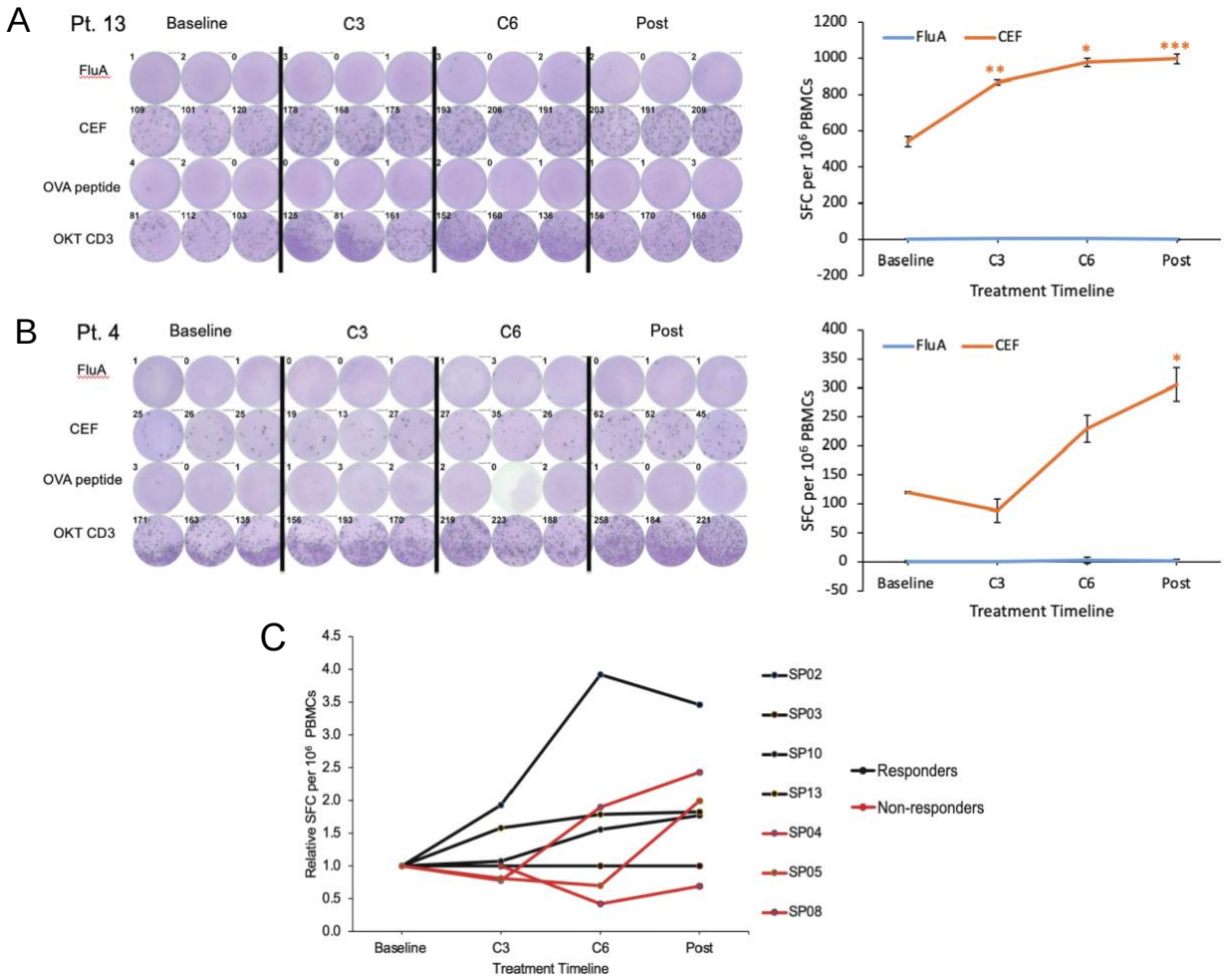

Figure 3. Standard of care first line platinum-based chemotherapy increased T cell responses to viral antigens following chemotherapy

(A, B) IFNγ ELISPOT responses to FluA and CEF peptide pool over the course of chemotherapy in patient 13 (chemo responder) and patient 4 (chemo non-responder). Spot forming cell (SFC) per 10^6 PBMCs were background (OVA)-subtracted with n = 3 biologically independent samples. Each data represents mean ± standard error of the mean (s.e.m.). Repeated-measures regression model with Dunnett's multiple comparison test was used for generating p values. $*P \leq 0.5$ $**P \leq 0.05$ $***P \leq 0.005$. **(C)** IFNγ ELISPOT responses to CEF peptide pool at each time point after chemotherapy relative to Baseline in all 7 patients.

Evaluation of T cell receptor (TCR) clonotype dynamics following chemotherapy

To gain insight into the mechanisms underlying increased T cell responses following chemotherapy, we sought to determine longitudinal changes of the T cell repertoire using bulk TCR sequencing. The bulk TCR sequencing read counts of the patient samples were heterogenous

with a median of 55170 reads per sample (range 3680 - 147180 reads) **(Figure 4A)**. We therefore evaluated the diversity of T cell repertoires throughout chemotherapy treatment by calculating a Normalized Shannon Index which measures T cell repertoire diversity by taking into account richness and evenness of T cell clones while correcting for the number of observations per sample **(Methods)**. Overall, the T cell repertoire diversity remained stable after chemotherapy (**Figure 4B and 4C**).

Given the overall stability of the T cell repertoires, we evaluated the dynamics of individual T cell clonotype in PBMCs of each of the 8 patients over four time points of chemotherapy (Baseline, C3, C6, and Post). By comparing the number of clones of each TCR clonotype between two consecutive chemotherapy stages, we categorized the TCR clonotypes into novel, expanded, disappeared, contracted, and unchanged for each patient **(Figure 4D)**. Expectedly, the percentage of changed T cell clonotypes was small after chemotherapy with a median of 2.9% of changed clonotypes per sample (range 0.7% - 34.7%). These dynamic clonotypes were more frequent amongst responding patients (**Figure 4E**), where we observed more novel and expanded TCR clonotypes from Baseline to C3 as well as more disappeared and contracted TCR clonotypes after C3 (**Figure 4F and 4G**). Finally, we focused on the dynamics of the most expanded clonotypes (n=100) in each patient assuming that these clones would represent antigen-experienced T cell clones (**Extended Data Figure 2A**). However, we did not detect clear patterns of change of these most expanded T cell clonotypes.

Altogether, the results of bulk TCR sequencing showed that overall T cell repertoires were stable following chemotherapy, albeit with a trend to higher turnover of clonotypes in chemo responders.

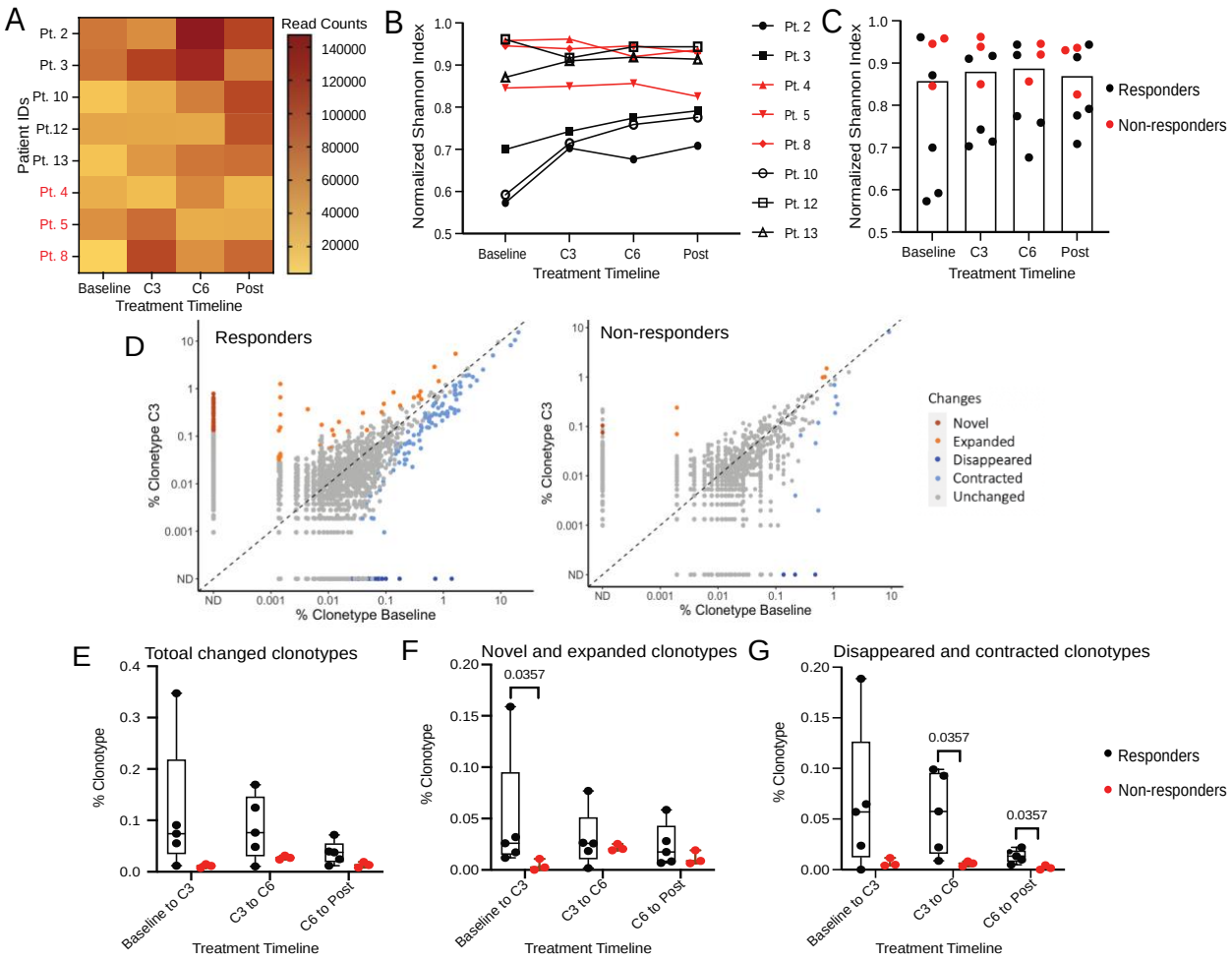

Figure 4. Changes of TCR clonotype proportions across the course of chemotherapy treatment (n = 8)

(A) Heatmap of read counts for samples of the 8 patients. **(B, C)** (B) Dynamics of the clonotype diversity for each patient over the course of chemotherapy. (C) Summary bar graph of the clonotype diversity of all samples over the course of chemotherapy. Each bar represents the median of each dataset. Clonotype diversity was represented using the Normalized Shannon Index by dividing the Shannon Index of each sample by its corresponding clonotype count. **(D)** Scatter plots of the individual clonotype dynamics between Baseline and the 3rd cycle of chemotherapy (C3). T cell clonotypes were defined based on CDR3 amino acid sequences of T cell β chain. Patients labeled in red were chemo non-responders and in black were chemo responders. Clonotypes of the 5 chemo responders (left) and 3 chemo non-responders (right) were combined, respectively. **(E-G)** Percentage of the overall changed clonotypes (E) or the novel and expended clonotypes (F) or the disappeared and shrunken clonotypes (G) between each two consecutive timepoint of chemotherapy treatment in chemo responders (n = 5) and non-responders (n = 3). Statistical analysis between chemo responders and non-responders was performed using two-sided Mann-Whitney U test without adjustment for multiple comparisons.

Chemotherapy leads to increased HLA class II expression on monocytes

To characterize the impact of platin-based chemotherapy on peripheral immune cell composition further, we performed single-cell RNA sequencing on PBMC samples of 4 responding patients (2, 3, 9, and 13) and 1 non-responding patient (4) collected before chemotherapy and after the third cycle of chemotherapy (C3). Immune cell populations were identified by marker gene expression **(Extended Data Figure 3A)** and composed of B cells, monocytes, dendritic cells (DCs), $CD4^+$ T cells, $CD8^+$ T cells and natural killer (NK) cells **(Figure 5A)**. To normalize the variations of the cell counts in patient samples and quantify the changes of immune cells after chemotherapy, the relative percentage of cells of each immune cell population was calculated **(Figure 5B and 5C)**. Patients 2, 3, 4 and 9 exhibited a trend to a higher frequency of monocytes after chemotherapy, which correlates to CBC measurements **(Figure 2D)**. Remarkably, the percentage of monocytes at C3 was more similar with healthy donor than at baseline for patients 2, 3, 4, and 9, which may suggest a recovery of monocyte populations after chemotherapy treatment **(Figure 5B)**. Moreover, all 5 patients demonstrated a decline in B cells **(Figure 5C)**. Finally, consistent with TCR bulk sequencing, the frequency of T cells remained stable **(Figure 5B and 5C)**.

Differential gene expression analysis of monocytes revealed upregulation of transcription factors such as *JUN* and *LYZ* as well as MHC class II genes after chemotherapy **(Figure 6A and 6B)**. The gene set enrichment analysis of the upregulated genes in C3 also indicated an increased antigen processing and presentation after chemotherapy **(Figure 6C and Extended Data Figure 4B)**. In sum, chemotherapy increased the antigen processing and presentation in monocytes but did not alter the percentage of T cells.

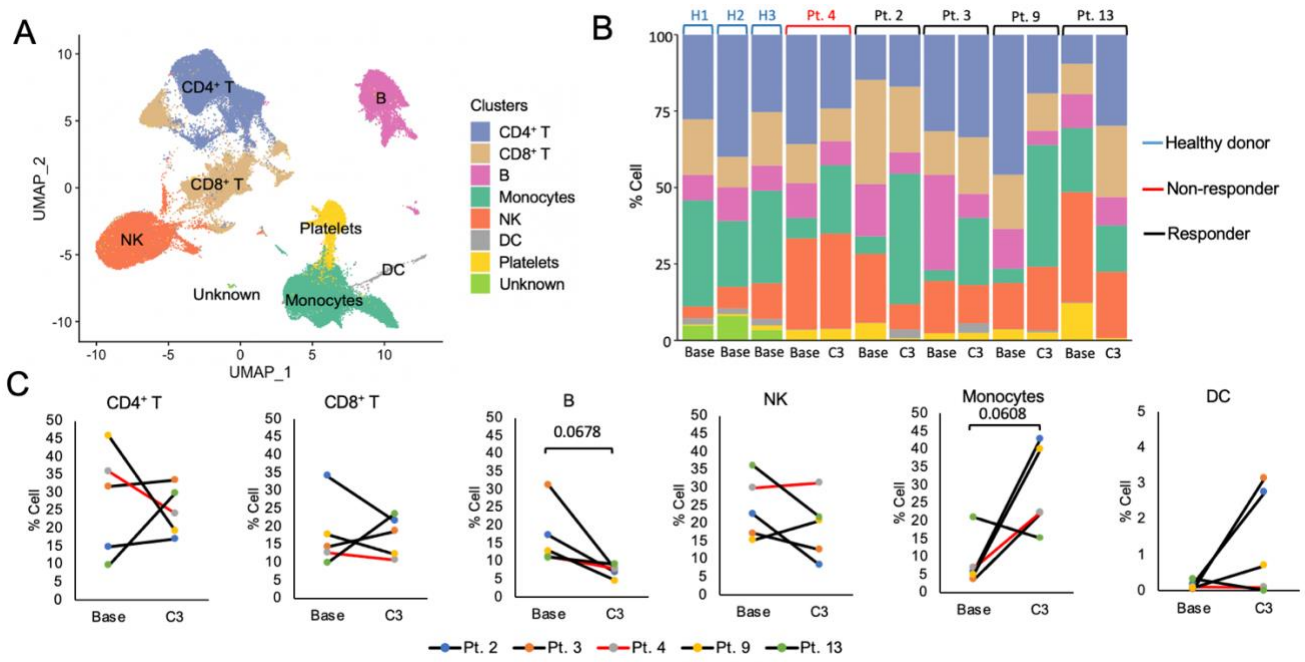

Figure 5. Dynamics of peripheral blood immune cell populations following chemotherapy **(A)** UMAP of the immune cell populations of the integrated PBMC samples from patient 2, 3, 4, 9, and 13. **(B)** The relative percentage of cells in each immune cell population. **(C)** Quantification of the percentage of cells pre-chemotherapy (Base) and after the third cycle of chemotherapy (C3). No statistical significance changes were detected between baseline and C3 using a one-sided t-test.

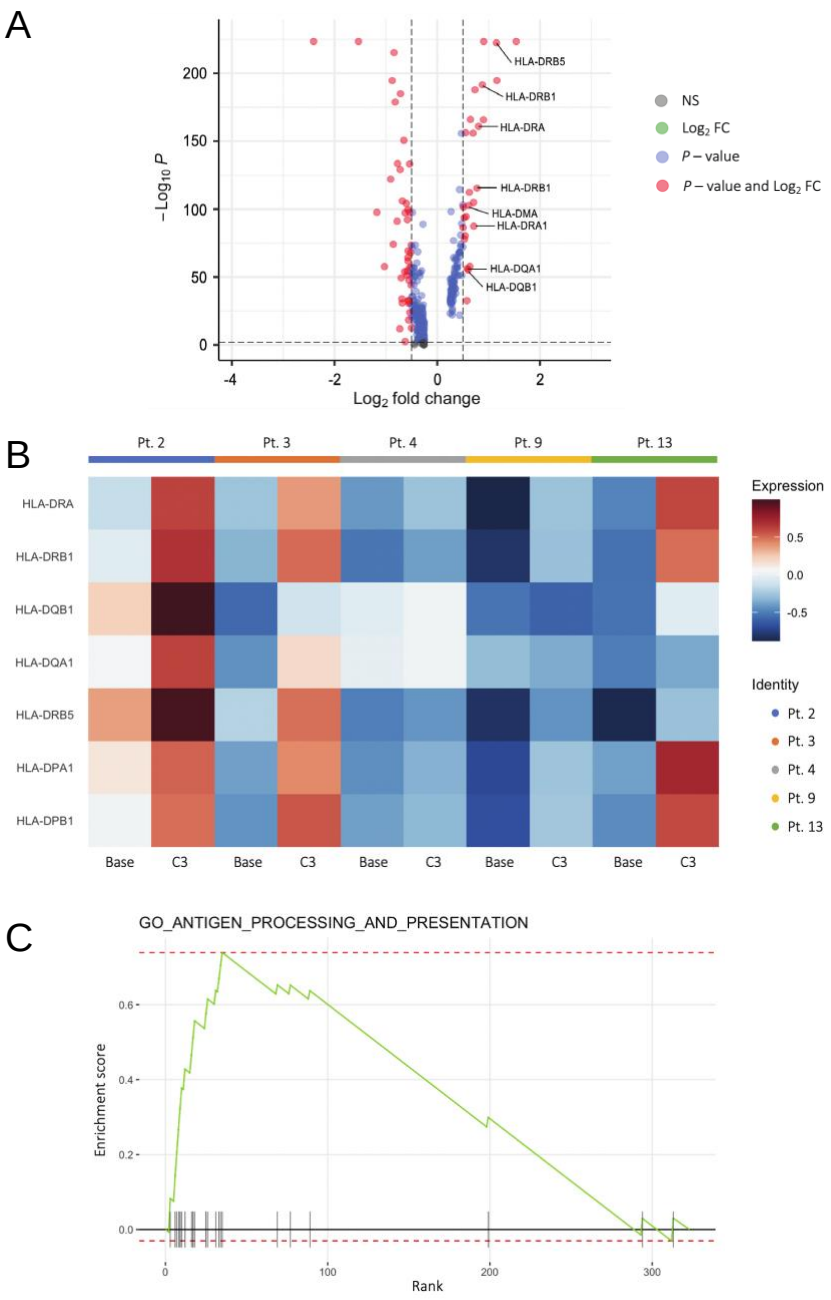

Figure 6. Differential gene expression analysis in monocytes after chemotherapy
(A) Differentially expressed genes between pre (Base) and the third cycle after chemotherapy (C3). Blue dots represented genes with false discovery rate-corrected P value < 0.01. Red dots represented genes with false discovery rate-corrected P value < 0.01 and log2 fold change > 0.5. **(B)** Differentially expressed HLA genes between Base and C3 in 5 patients with false discovery rate-corrected P value < 0.01 and log2 fold change > 0.5. **(C)** Enrichment score of the identified upregulated genes at C3 overlapped with the gene set in the antigen processing and presentation pathway with significant false discovery rate-corrected q-values < 0.05. Positive values indicated the upregulated genes after the third cycle of chemotherapy.

Phenotypic changes of TCR clonotypes following chemotherapy

To link the TCR clonotypes with their corresponding phenotypes for each individual T cell, we mapped TCR clonotypes of patients 2, 3, 4, 9, and 13 to each of the $CD8^+$ and $CD4^+$ T cell states using single-cell TCR sequencing. To overcome batch effects, samples were integrated and $CD8^+$ and $CD4^+$ T cell subclusters were annotated using a PBMC reference dataset **(Figure 7A and Methods)**. The predicted $CD8^+$ T cell states were verified with characteristic gene signatures **(Extended Data Figure 5A)**, for example *MKI67* and *EOMES* (proliferating $CD8^+$ T cells); *SELL*, *CCR7*, *IL7R*, *CD27*, and *TCF7* (naïve $CD8^+$ T cells); *ILR7* and TCF7 (central memory $CD8^+$ T cells or TCM); granzymes, granulysin, and KLRG1 (effector memory $CD8^+$ T cells or TEM). MAIT cells demonstrated known restricted diversity of TCR alpha chains and harbored published CDR3α and CDR3β sequences[69].

In order to access changes of T cell clones, TCR clonotypes were categorized as either multitons or singletons. TCR clonotypes that expanded in multiple T cells were defined as multitons while TCR clonotypes found in a single T cell were characterized as singletons. By visualizing the compositions of clonotype in each $CD8^+$ T cell subcluster, we observed a higher proportion of singleton in the naïve and central memory $CD8^+$ T cell population and a higher proportion of multitons in the proliferating, effector memory, and MAIT subclusters **(Figure 7B)**. Evaluation of the TCR clonotype frequency also demonstrated that $CD8^+$ T cells with effector memory state were composed by more expanded TCR clonotypes **(Figure 7C)**. The composition of $CD8^+$ T cell clonotypes suggested that most of the naïve T cells had a unique TCR clonotype while majority of the expanded T cells had effector memory phenotype.

Before accessing the changes of TCR clonotypes after chemotherapy, we first compared the TCR clonotypes in the single T cell with bulk TCR sequencing data and found good correlation with a large proportion of TCR clonotypes identified at similar frequency by both methods. Interestingly, most of the TCR clonotypes detected by both methods were effector memory $CD8^+$ T cells or MAIT, which is likely a result of these cells being more expanded than other T cell subpopulations and therefore they have a higher chance of being detected using TCR sequencing **(Extended Data Figure 6B)**.

To determine whether chemotherapy altered the functional states of $CD8^+$ TCR clonotypes and if there were distinct changing patterns between chemo responders and non-responders, we evaluated the dynamics of clonotypes by patients and by T cell subclusters **(Figure 7E and 7F)**. TCR clonotypes of all $CD8^+$ T cell states were stable in patients 2, 3, and 4. In patient 9, the percentage of $CD8^+$ TCR clonotype with naïve phenotype decreased after the third cycle of chemotherapy while percent $CD8^+$ TCR clonotype in effector memory population increased. Patient 13, however, had opposite changing pattern of the percent clonotype in naïve and effector memory $CD8^+$ T cell populations as patient 9. Thus, no distinct patterns were observed between chemo responders and non-responder. Heterogeneous changing patterns of $CD8^+$ T cell were observed **(Figure 7E)** with a trend towards elevated percentage in central memory $CD8^+$ T cell clonotype after chemotherapy **(Figure 7F)**, which suggested a potential for chemotherapy to stimulate the TCR clonotype diversity in central memory $CD8^+$ T cell population.

$CD4^+$ T cells also exhibited diverse subpopulations according to the predicted T cell states and gene signatures upregulated in each cluster, such as *MKI67* in proliferating $CD4^+$ T cells; *CCR7*

and *TCF7* in naïve $CD4^+$ T cells; *CCR7* and *S100A4* in central memory $CD4^+$ T cells (TCM); *GZMA*, *GZMK*, *KLRB1*, and *KLRG1* in effector memory $CD4^+$ T cells (TEM); granzymes and granulysin in cytotoxic $CD4^+$ T cell (CTL); and *FOXP3* and *CTLA4* in regulatory T cells (Treg) **(Figure 8A and Extended Data Figure 5B)**. Similar to $CD8^+$ T cell clonotypes, the changes of the percentage of $CD4^+$ T cell subclusters were heterogenous among patients **(Figure 8E)** but with an increased trend in the percentage of $CD4^+$ T cell clonotypes after chemotherapy **(Figure 8F)**. Nevertheless, no significant transcriptional change was observed in regulatory $CD4^+$ T cells after chemotherapy.

Altogether, the percent clonotypes were stable in $CD8^+$ and $CD4^+$ T cell populations after chemotherapy in all 5 patients. Chemotherapy could, however, induce trends towards increased central memory $CD8^+$ and regulatory $CD4^+$ T cells after the first 3 cycles of chemotherapy. In addition, there were no changing patterns for chemo responders and non-responders in both $CD8^+$ and $CD4^+$ T cell subpopulations.

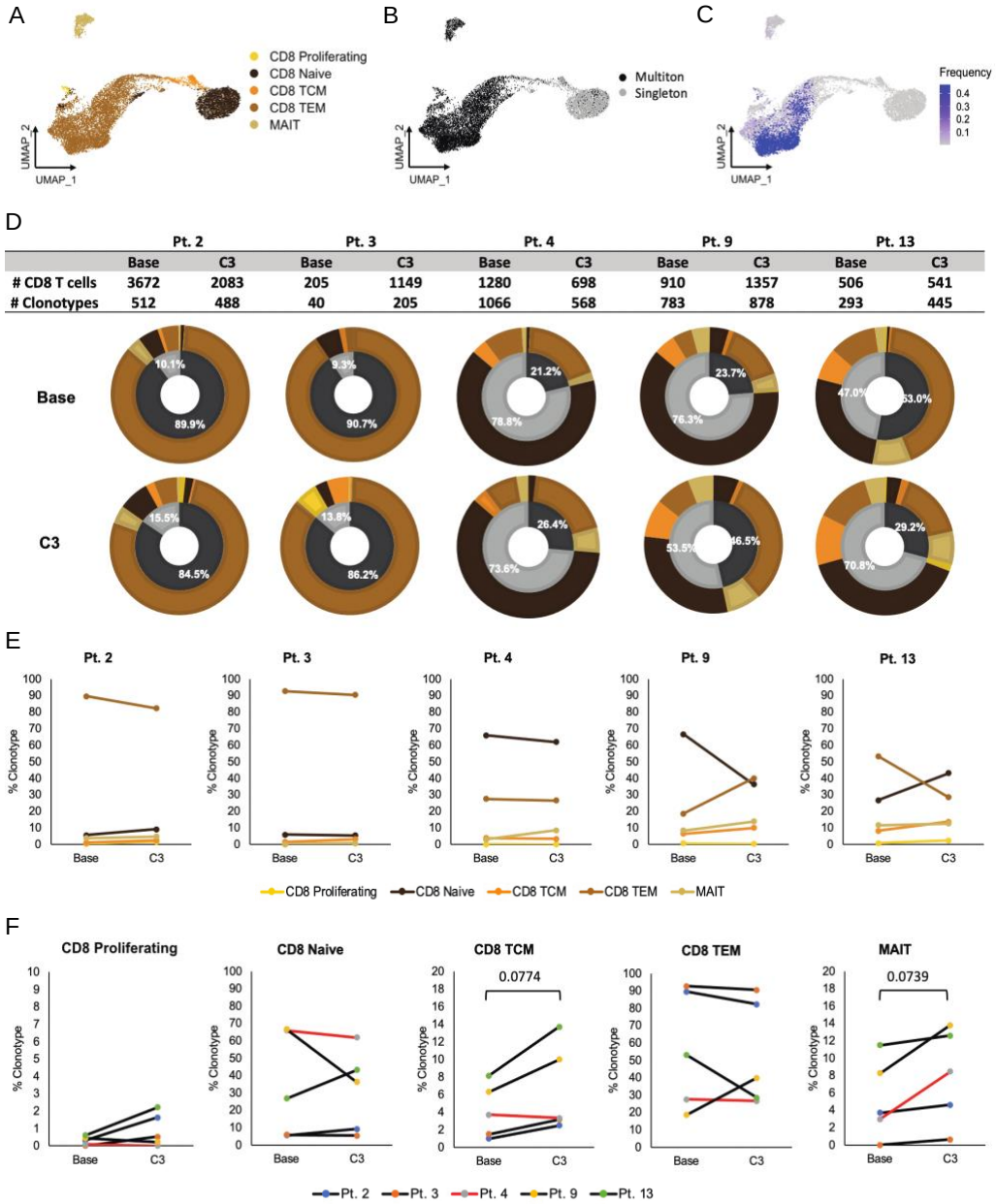

Figure 7. Stability of CD8⁺ T cell subpopulations following chemotherapy
(A) UMAP of the CD8⁺ T cell sub-populations of 5 patients (Pt.2, Pt.3, Pt.4, Pt.9, and Pt.13). **(B)** Distribution of the multitons and singletons of the CD8⁺ T cell clonotypes. **(C)** Frequency map of the CD8⁺ T cell clonotypes. The frequency of each T cell clonotype was calculated within each sample. **(D)** Summary table of the number of CD8⁺ T cells and clonotypes in each of the 5 patients pre- and after 3 cycles of chemotherapy. Pie charts percentages of multitons and singletons in proliferating, naïve, central memory (TCM), effector memory (TEM), and Mucosal-associated invariant (MAIT) T cell states. **(E)** Changes of percent clonotype of proliferating, naïve, TEM, TCM CD8⁺ T cell and MAIT sub-clusters in each of the 5 patients after the third cycle of chemotherapy. **(F)** Changes of percent clonotype of 5 patients in proliferating, naïve, TEM, TCM CD8⁺ T cell and MAIT sub-clusters after the third cycle of chemotherapy. *P*-values were calculated using one-sample t-test.

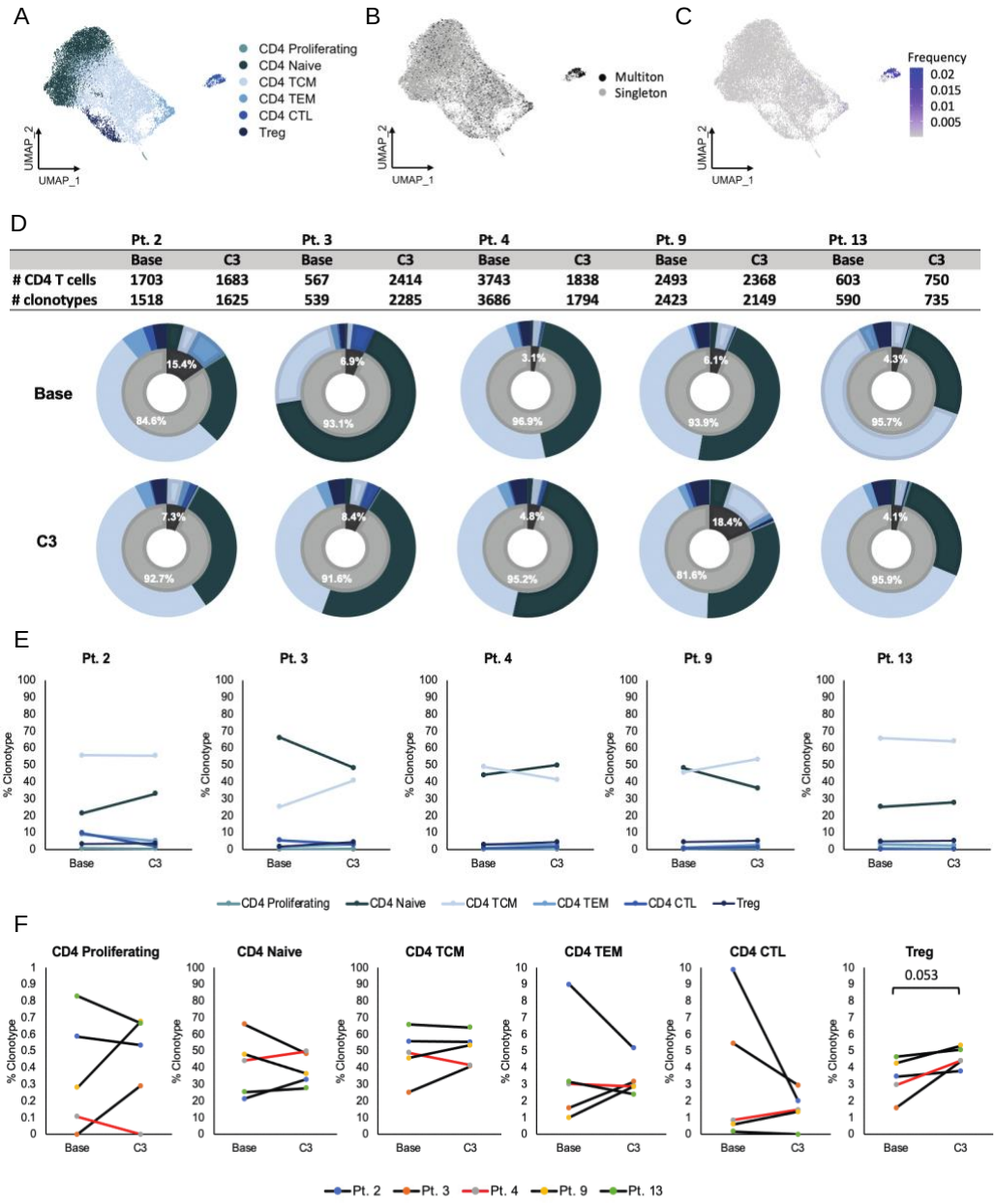

Figure 8. Increase of regulatory T cells following chemotherapy

(A) UMAP of the CD4$^+$ T cell sub-populations of 5 patients (Pt.2, Pt.3, Pt.4, Pt.9, and Pt.13). **(B)** Distribution of the multitons and singletons of the CD4$^+$ T cell clonotypes. **(C)** Frequency map of the CD4$^+$ T cell clonotypes. The frequency of each T cell clonotype was calculated within each sample. **(D)** Summary table of the number of CD4$^+$ T cells and clonotypes in each of the 5 patients pre- and after 3 cycles of chemotherapy. Pie charts percentages of multitons and singletons in proliferating, naïve, central memory (TCM), effector memory (TEM), cytotoxic (CTL), and regulatory CD4$^+$ T cell (Treg) states. **(E)** Changes of percent clonotype in proliferating, naïve, TCM, TEM, CTL, and Treg sub-clusters in each of the 5 patients after the third cycle of chemotherapy. **(F)** Changes of percent clonotype of 5 patients in proliferating, naïve, TCM, TEM, CTL, and Treg sub-clusters after the third cycle of chemotherapy. *P*-values were calculated using one-sample t-test.

Chapter 3: Discussion and Perspectives

Discussion

Epithelial ovarian cancer (EOC) is the one of the most lethal gynecological cancer worldwide. Current first-line treatment approaches for EOC include primary debulking surgery and chemotherapy. Platinum- and taxane-based chemotherapy is able to control the growth of ovarian cancer cells. However, the impact of chemotherapy on patients' peripheral immune responses are largely unknown. Thus, our study aimed to understand the changes of immune status and composition of circulating immune cells following chemotherapy.

In this study, we assessed T cell responses to viral antigens at baseline, after three and six cycles of chemotherapy and at a follow-up after 2 months. We observed improved response to viral antigens after chemotherapy in all patients. The responses were more pronounced in patients who had initially responded to chemotherapy, which is consistent with the higher reduction of tumor burden indicated by CA125 level. Bulk TCR sequencing allowed further dissection of TCR repertoires throughout chemotherapy. We found stable TCR repertoire diversities across the course of chemotherapy with a larger proportion of changed clonotypes in chemo responders. The single cell TCR sequencing also demonstrated stability of percent T cell clonotype in most of the T cell subpopulations, except trends towards increased central memory CD8+ and regulatory T cells regardless of response status. We also noticed an upward trend in circulating monocytes and higher HLA class II expression after chemotherapy, which suggested a potential of chemotherapy in inducing antigen processing and presentation by monocytes.

With respect to why there were increases in T cell responses to viral antigens and increased trends in memory TCR clonotypes, one possibility could be reinvigoration of suppressed effector and memory T cell populations due to reduced tumor burden during chemotherapy. Previous studies have shown that cross-reactivity to similar epitopes derived from other microbial genomes may elicit effector and memory T cell populations against viral antigens that individuals may not have encountered[70]. Thus, the result of increased T cell response to influenza and CEF peptide pool may not be solely due to viral infection but could be the cross-reactivity of epitopes from other microbes, which also explains the upward trend in memory T cell population in the single-cell analysis. Another possibility of the increased trend in memory T cell population could be the homeostatic proliferation of T cells after chemotherapy. The proliferating T cells that existed before chemotherapy may acquire the memory phenotypes during the clonal evolution induced by the standard care of chemotherapy treatment.

To identify the specificities of the TCR clonotypes detected in patients' peripheral samples, we mapped the CDR3 amino acid sequences of TCR α and/or β chains from both the bulk and single-cell TCR sequencing of our patients to the CDR3 amino acid sequences of TCR α and/or β chains in the publicly available datasets (VDJdb and McPAS-TCR)[62,63]. Neoantigen-specific epitopes were annotated with matched CDR3 amino acid sequence of either TCR α and/or β, and none of the neoantigen specific TCR clonotypes were found with matched TCR α and β chains in the databases. Several significantly changed TCR clonotypes in bulk TCR sequencing were annotated as viral (including cytomegalovirus, Epstein Barr virus, influenza, and M.Tuberculosis) and autoimmune disease (including established rheumatoid arthritis and autologous transplantation for multiple sclerosis) specific epitopes.

Our analysis demonstrated an elevation of HLA class II expression and antigen presentation in monocyte populations, which we interpret as result of chemotherapy. An open question is the mechanism of enhanced HLA class II expression on monocytes. It has been shown that chemotherapy-induced immunogenic cell death (ICD) and the release of tumor-associated antigens can increase the expression of calreticulin on the tumor cell surface and may promote phagocytic uptake of cancer cells, which could further increase antigen cross-presentation, thus facilitating the infiltration of activated cytotoxic T cells in the tumor microenvironment[71]. It is possible that the upregulations of HLA expression and increased antigen presentation in peripheral monotypes of our patients results from increased tumor associated antigens induced by chemotherapy administration. Furthermore, previous report indicated that platinum-based chemotherapy may alter monocyte differentiation and drive macrophages towards a M2-like phenotype in the tumor microenvironment. However, the transition from M1-like to M2-like signatures was not observed in the peripheral monocytes in our patient cohort[72].

Single cell sequencing technologies have been applied in various malignancies including melanoma, glioblastoma and breast cancer[60,73,74]. Single cell RNA sequencing is now also increasingly used in ovarian cancer to address questions related to tumor subtypes, evolution and treatments. A single cell landscape of ovarian cancer patients, investigated by Izar and colleagues, demonstrated intra and inter-patient variations of the tumor and immune cells in the ascites ecosystem[75]. Izar and colleagues also showed that despite the intra-patient heterogeneity, the expression of MHC class II in subsets of malignant cells were consistent across multiple patients and may be involved in increasing tumor-infiltrating lymphocytes, prognosis, and treatment response[75]. Similarly, we also observed heterogeneous changing patterns of circulating immune

cells but with an upward trend in HLA class II expression and antigen presentation in circulating monocytes after chemotherapy in the majority of our patients. Thus, interconnections between malignant and non-malignant compartment as well as circulating immune cells may occur during co-evolution and treatment. Nevertheless, variations between tumor infiltrating lymphocytes (TILs) and circulating immune cells may also exist. For example, previous neoadjuvant chemotherapy studies in patients demonstrated an increased density of $CD8^+$ TILs [30,76,77] and PD-1^+ T cells in the tumor microenvironment after treatment[30]. In the present study, however, neither the increase of $CD8^+$ T cells nor PD-L1/PD-1 expression was observed in the circulating T cells. These observations point to difference between immune cells residing in the tumor microenvironment and circulating populations. Comparative studies of matched tumor and peripheral blood samples are needed to understand the differences between tumor-infiltrating immune cells and those present in peripheral blood.

Limitations

Although this study provided insights into circulating immune responses during chemotherapy treatment, there are several limitations. Firstly, a limited number of immune cells, including $CD8^+$ and $CD4^+$ T cells, were sampled and studied in bulk and single-cell analysis. Thus, the immune cells and T cell clonotypes obtained during the sampling process may not fully reflect the composition and behavior of the entire immune cell repertoire in patients involved in this study. Therefore, it is possible that discrepancies among patients and at the different treatment timelines were due to technical artifacts or sampling variations rather than biological differences. Secondly, the T cell clonotype annotation was limited due to the high diversity of antigen epitopes, such as mutations of viral and tumor genomes. The potential of T cell cross-reactivity with environmental

antigens increased the difficulty of predicting T cell specificities. Since bulk TCR-seq does not provide paired TCR α/β sequences, annotation of T cell clonotypes has to be performed separately for both TCR chains and therefore remains incomplete. For example, the CDR3 amino acid sequence of α and β chains of a single T cell could map to multiple antigen epitopes that T cell recognized in the public annotation databases. It is hard to ensure that a certain antigen epitope was recognized by the corresponding individual T cell clonotype. Another caveat for the publicly available datasets used in this study is the limited neoantigen-specific epitopes for ovarian cancer. Most of the documented neoantigen epitopes are from melanoma, liver, or lung cancer. Thirdly, diversity analysis using the Shannon index may not be able to account for the similarity of each CDR3 amino acid or nucleotide sequence. Thus, clonal relatedness of T cell clonotypes may not be captured. For single-cell RNA sequencing analysis, the inter-patient heterogeneity also led to difficulties in marker identifications and cell type annotations, which restricted the in-depth distinctions among immune cell subpopulations, especially in T cell subclusters. In addition, the lack of significant changes before and after chemotherapy may be due to our smaller sample size.

Future directions

Despite the limitation in this study, exploring the responses of circulating immune cells still provided additional information for understanding the dynamics of host immune responses under the pressure of chemotherapy for EOC patients. The mechanisms of circulating and tumor-infiltrating immune cells against solid tumor over the course of cancer therapy remains a field that requires future investigation. Clonal evolution of the tumor may occur during chemotherapy. Thus, the identifications of neoantigen-specific TCR clonotypes are helpful for tracking the clonality alternations and evolution of neoantigen-specific T cells over the course of chemotherapy, which

may serve as potential indicators or biomarkers for monitoring patients' responses to chemotherapy. In addition, matching the TCR clonotypes in the peripheral blood sample with the predicted neoantigen epitopes from the tumor specimen may further distinguish the tumor-specific and bystander T cell populations in the circulation and better understand the correlation between circulating and tumor-infiltrating lymphocytes. With the rapid development and application of sequencing techniques, comprehensive muti-omics studies of tumor and immune cells may be helpful for understanding of resistance evolution in response to therapy, investigating metastatic dissemination and circulating tumor cells, and identifying differential expression patterns of tumor and immune cells between responders and non-responders in ovarian cancer patients. Altogether, understanding the mechanisms of neoantigen-specific T cell dynamics in response to chemotherapy could provide additional information for the construction and administration timeline of personalized neoantigen vaccine for patients with epithelial ovarian cancer.

Chapter 4: Bibliography

1. Siegel, R. L., Miller, K. D., Fuchs, H. E. & Jemal, A. Cancer Statistics, 2021. *CA: A Cancer Journal for Clinicians* **71**, 7–33 (2021).
2. DeVita, V. T. & Chu, E. A history of cancer chemotherapy. *Cancer Research* vol. 68 8643–8653 (2008).
3. Oza md, A. *et al. S20 Current OnCOlOgy-VOlume 18, Supplement 2 Progression-free survival in advanced ovarian cancer: a Canadian review and expert panel perspective*. (2011).
4. Essel, K. G. *et al.* PARPi after PARPi in epithelial ovarian cancer. *Gynecologic Oncology Reports* **35**, (2021).
5. Shoji *et al.* A New Therapeutic Strategy for Recurrent Ovarian Cancer—Bevacizumab beyond Progressive Disease. *Healthcare* **7**, 109 (2019).
6. Krause-Heuer, A. M. *et al.* Studies of the mechanism of action of platinum(II) complexes with potent cytotoxicity in human cancer cells. *Journal of Medicinal Chemistry* **52**, 5474–5484 (2009).
7. Mikuła-Pietrasik, J. *et al.* Comprehensive review on how platinum- and taxane-based chemotherapy of ovarian cancer affects biology of normal cells. *Cellular and Molecular Life Sciences* vol. 76 681–697 (2019).
8. Fitzpatrick, J. M. & de Wit, R. Taxane mechanisms of action: Potential implications for treatment sequencing in metastatic castration-resistant prostate cancer. *European Urology* **65**, 1198–1204 (2014).
9. National Cancer Institute. *Cancer Stat Facts: Ovarian Cancer.* (2021).
10. Torre, L. A. *et al.* Ovarian cancer statistics, 2018. *CA: A Cancer Journal for Clinicians* **68**, 284–296 (2018).
11. Ryland, G. L. *et al.* Mutational landscape of mucinous ovarian carcinoma and its neoplastic precursors. *Genome Medicine* **7**, (2015).
12. Vang, R. *et al.* Molecular alterations of TP53 are a defining feature of ovarian high-grade serous carcinoma: A rereview of cases lacking tp53 mutations in the cancer genome atlas ovarian study. *International Journal of Gynecological Pathology* **35**, 48–55 (2016).
13. Ramus, S. J. & Gayther, S. A. The Contribution of BRCA1 and BRCA2 to Ovarian Cancer. *Molecular Oncology* vol. 3 138–150 (2009).
14. Cannistra, S. A. *Cancer of the Ovary*. www.nejm.org.
15. Gantner, P. *et al.* Single-cell TCR sequencing reveals phenotypically diverse clonally expanded cells harboring inducible HIV proviruses during ART. *Nature Communications* **11**, (2020).
16. Mikuła-Pietrasik, J. *et al.* Comprehensive review on how platinum- and taxane-based chemotherapy of ovarian cancer affects biology of normal cells. *Cellular and Molecular Life Sciences* vol. 76 681–697 (2019).
17. Ozols, R. F. Systemic Therapy for Ovarian Cancer: Current Status and New Treatments. *Seminars in Oncology* **33**, 3–11 (2006).
18. Piccart, M. J. *et al. Randomized Intergroup Trial of Cisplatin-Paclitaxel Versus Cisplatin-Cyclophosphamide in Women With Advanced Epithelial Ovarian Cancer: Three-Year Results*. https://academic.oup.com/jnci/article/92/9/699/2906130.

19. Kuroki, L. & Guntupalli, S. R. Treatment of epithelial ovarian cancer. *The BMJ* vol. 371 (2020).
20. Pignata, S., Cecere, S. C., du Bois, A., Harter, P. & Heitz, F. Treatment of recurrent ovarian cancer. *Annals of Oncology* **28**, viii51–viii56 (2017).
21. Charles, A., Dewayani, B. M., Sahiratmadja, E., Winarno, G. N. A. & Susanto, H. Paclitaxel-carboplatin chemotherapy induced hematologic toxicities among epithelial ovarian cancer patients. *Universa Medicina* **35**, 165 (2016).
22. Dunton, C. J. Management of Treatment-Related Toxicity in Advanced Ovarian Cancer. *The Oncologist* **7**, 11–19 (2002).
23. Jayson, G. C., Kohn, E. C., Kitchener, H. C. & Ledermann, J. A. Ovarian cancer. *The Lancet* vol. 384 1376–1388 (2014).
24. Bast C. R. *et al.* A radioimmunoassay using a monoclonal antibody to monitor the course of epithelial ovarian cancer. *The New England Journal of Medicine* **309**, 884-887 (1983).
25. Samadi Pakchin, P., Fathi, M., Ghanbari, H., Saber, R. & Omidi, Y. A novel electrochemical immunosensor for ultrasensitive detection of CA125 in ovarian cancer. *Biosensors and Bioelectronics* **153**, (2020).
26. Feng, L. Y., Liao, S. bin & Li, L. Preoperative serum levels of HE4 and CA125 predict primary optimal cytoreduction in advanced epithelial ovarian cancer: A preliminary model study. *Journal of Ovarian Research* **13**, (2020).
27. Kessous, R. *et al.* CA-125 reduction during neoadjuvant chemotherapy is associated with success of cytoreductive surgery and outcome of patients with advanced high-grade ovarian cancer. *Acta Obstetricia et Gynecologica Scandinavica* **99**, 933–940 (2020).
28. Markman, M., Federico, M., Liu, P. Y., Hannigan, E. & Alberts, D. Significance of early changes in the serum CA-125 antigen level on overall survival in advanced ovarian cancer. *Gynecologic Oncology* **103**, 195–198 (2006).
29. Peng, J. *et al.* Chemotherapy induces programmed cell death-ligand 1 overexpression via the nuclear factor-κBto foster an immunosuppressive tumor microenvironment in Ovarian Cancer. *Cancer Research* **75**, 5034–5045 (2015).
30. Lo, C. S. *et al.* Neoadjuvant chemotherapy of ovarian cancer results in three patterns of tumor-infiltrating lymphocyte response with distinct implications for immunotherapy. *Clinical Cancer Research* **23**, 925–934 (2017).
31. Zhang, L. *et al.* Differential impairment of regulatory T cells rather than effector T cells by paclitaxel-based chemotherapy. *Clinical Immunology* **129**, 219–229 (2008).
32. Kodumudi, K. N. *et al.* A novel chemoimmunomodulating property of docetaxel: Suppression of myeloid-derived suppressor cells in tumor bearers. *Clinical Cancer Research* **16**, 4583–4594 (2010).
33. Mouw, K. W., Goldberg, M. S., Konstantinopoulos, P. A. & D'Andrea, A. D. DNA damage and repair biomarkers of immunotherapy response. *Cancer Discovery* vol. 7 675–693 (2017).
34. Khairallah, A. S., Genestie, C., Auguste, A. & Leary, A. Impact of neoadjuvant chemotherapy on the immune microenvironment in advanced epithelial ovarian cancer: Prognostic and therapeutic implications. *International Journal of Cancer* vol. 143 8–15 (2018).
35. Melhem, A. *et al.* Administration of glucocorticoids to ovarian cancer patients is associated with expression of the anti-apoptotic genes SGK1 and MKP1/DUSP1 in ovarian tissues. *Clinical Cancer Research* **15**, 3196–3204 (2009).

36. Cassileth, P. A. *et al. Antiemetic Efficacy of Dexamethasone Therapy in Patients Receiving Cancer Chemotherapy*. https://jamanetwork.com/.
37. Chen, Y. X. *et al.* Dexamethasone enhances cell resistance to chemotherapy by increasing adhesion to extracellular matrix in human ovarian cancer cells. *Endocrine-Related Cancer* **17**, 39–50 (2010).
38. Meehan, R. S. & Chen, A. P. New treatment option for ovarian cancer: PARP inhibitors. *Gynecologic Oncology Research and Practice* **3**, (2016).
39. Liu, J. F., Konstantinopoulos, P. A. & Matulonis, U. A. PARP inhibitors in ovarian cancer: Current status and future promise. *Gynecologic Oncology* vol. 133 362–369 (2014).
40. Lee, E. K. & Konstantinopoulos, P. A. PARP inhibition and immune modulation: scientific rationale and perspectives for the treatment of gynecologic cancers. *Therapeutic Advances in Medical Oncology* vol. 12 (2020).
41. Borella, F. *et al.* Immune checkpoint inhibitors in epithelial ovarian cancer: An overview on efficacy and future perspectives. *Diagnostics* vol. 10 (2020).
42. Färkkilä, A. *et al.* Immunogenomic profiling determines responses to combined PARP and PD-1 inhibition in ovarian cancer. *Nature Communications* **11**, (2020).
43. Corcoran, R. B. Liquid biopsy versus tumor biopsy for clinical-trial recruitment. *Nature Medicine* vol. 26 1815–1816 (2020).
44. Russano, M. *et al.* Liquid biopsy and tumor heterogeneity in metastatic solid tumors: The potentiality of blood samples. *Journal of Experimental and Clinical Cancer Research* vol. 39 (2020).
45. Nixon, A. B. *et al.* Peripheral immune-based biomarkers in cancer immunotherapy: can we realize their predictive potential? *Journal for ImmunoTherapy of Cancer* vol. 7 (2019).
46. Pawelec, G., Verschoor, C. P. & Ostrand-Rosenberg, S. Myeloid-derived suppressor cells: Not only in tumor immunity. *Frontiers in Immunology* vol. 10 (2019).
47. Heather, J. M. & Chain, B. The sequence of sequencers: The history of sequencing DNA. *Genomics* vol. 107 1–8 (2016).
48. Schatz, M. C. Biological data sciences in genome research. *Genome Research* vol. 25 1417–1422 (2015).
49. Stark, R., Grzelak, M. & Hadfield, J. RNA sequencing: the teenage years. *Nature Reviews Genetics* vol. 20 631–656 (2019).
50. Chattopadhyay, P. K., Gierahn, T. M., Roederer, M. & Love, J. C. Single-cell technologies for monitoring immune systems. *Nature Immunology* vol. 15 128–135 (2014).
51. Zhang, X. *et al.* Comparative Analysis of Droplet-Based Ultra-High-Throughput Single-Cell RNA-Seq Systems. *Molecular Cell* **73**, 130-142.e5 (2019).
52. Yamawaki, T. M. *et al.* Systematic comparison of high-throughput single-cell RNA-seq methods for immune cell profiling. *BMC Genomics* **22**, (2021).
53. de Simone, M., Rossetti, G. & Pagani, M. Single cell T cell receptor sequencing: Techniques and future challenges. *Frontiers in Immunology* vol. 9 (2018).
54. Schultze, J. L. Teaching "big data" analysis to young immunologists. *Nature Immunology* vol. 16 902–905 (2015).
55. Vieth, B., Parekh, S., Ziegenhain, C., Enard, W. & Hellmann, I. A systematic evaluation of single cell RNA-seq analysis pipelines. *Nature Communications* **10**, (2019).
56. Chen, Y. *et al. edgeR: differential analysis of sequence read count data User's Guide*.

57. Duò, A., Robinson, M. D. & Soneson, C. A systematic performance evaluation of clustering methods for single-cell RNA-seq data. *F1000Research* **7**, 1141 (2018).
58. Li, S. *et al.* RNase H–dependent PCR-enabled T-cell receptor sequencing for highly specific and efficient targeted sequencing of T-cell receptor mRNA for single-cell and repertoire analysis. *Nature Protocols* **14**, 2571–2594 (2019).
59. van Ingen, H. E. *et al. Analytical and clinical evaluation of an electrochemiluminescence immunoassay for the determination of CA 125*. https://academic.oup.com/clinchem/article/44/12/2530/5643134.
60. Hu, Z. *et al.* Personal neoantigen vaccines induce persistent memory T cell responses and epitope spreading in patients with melanoma. *Nature Medicine* (2021) doi:10.1038/s41591-020-01206-4.
61. Rempala, G. A. & Seweryn, M. Methods for diversity and overlap analysis in T-cell receptor populations. *Journal of Mathematical Biology* **67**, 1339–1368 (2013).
62. Bagaev, D. v. *et al.* VDJdb in 2019: Database extension, new analysis infrastructure and a T-cell receptor motif compendium. *Nucleic Acids Research* **48**, D1057–D1062 (2020).
63. Tickotsky, N., Sagiv, T., Prilusky, J., Shifrut, E. & Friedman, N. McPAS-TCR: A manually curated catalogue of pathology-associated T cell receptor sequences. *Bioinformatics* **33**, 2924–2929 (2017).
64. Stuart, T. *et al.* Comprehensive Integration of Single-Cell Data. *Cell* **177**, 1888-1902.e21 (2019).
65. Hao, Y. *et al.* Integrated analysis of multimodal single-cell data. *bioRxiv* (2020) doi:10.1101/2020.10.12.335331.
66. Chen, Y. *et al.* Baseline and post prophylactic tubal-ovarian surgery CA125 levels in BRCA1 and BRCA2 mutation carriers. *Familial Cancer* **13**, 197–203 (2014).
67. Kim, Y. J. *et al.* Pretreatment neutrophil-to-lymphocyte ratio and its dynamic change during neoadjuvant chemotherapy as poor prognostic factors in advanced ovarian cancer. *Obstetrics and Gynecology Science* **61**, 227–234 (2018).
68. Bernal-Estévez, D., Sánchez, R., Tejada, R. E. & Parra-López, C. Chemotherapy and radiation therapy elicits tumor specific T cell responses in a breast cancer patient. *BMC Cancer* **16**, (2016).
69. Mori, L., Lepore, M. & de Libero, G. The Immunology of CD1- and MR1-Restricted T Cells. *Annual Review of Immunology* vol. 34 479–510 (2016).
70. Su, L. F., Kidd, B. A., Han, A., Kotzin, J. J. & Davis, M. M. Virus-Specific CD4+ Memory-Phenotype T Cells Are Abundant in Unexposed Adults. *Immunity* **38**, 373–383 (2013).
71. Hannani, D. *et al.* Prerequisites for the Antitumor Vaccine-Like Effect of Chemotherapy and Radiotherapy. *The Cancer Journal &* **17**,.
72. Dijkgraaf, E. M. *et al.* Chemotherapy alters monocyte differentiation to favor generation of cancer-supporting m2 macrophages in the tumor microenvironment. *Cancer Research* **73**, 2480–2492 (2013).
73. Keskin, D. B. *et al.* Neoantigen vaccine generates intratumoral T cell responses in phase Ib glioblastoma trial. *Nature* **565**, 234–239 (2019).
74. Almendro, V. *et al.* Inference of tumor evolution during chemotherapy by computational modeling and in situ analysis of genetic and phenotypic cellular diversity. *Cell Reports* **6**, 514–527 (2014).

75. Izar, B. *et al.* A single-cell landscape of high-grade serous ovarian cancer. *Nature Medicine* **26**, 1271–1279 (2020).
76. Wouters, M. C. A. *et al.* Treatment regimen, surgical outcome, and t-cell differentiation influence prognostic benefit of tumor-infiltrating lymphocytes in high-grade serous ovarian cancer. *Clinical Cancer Research* **22**, 714–724 (2016).
77. Böhm, S. *et al.* Neoadjuvant chemotherapy modulates the immune microenvironment in metastases of tubo-ovarian high-grade serous carcinoma. *Clinical Cancer Research* **22**, 3025–3036 (2016).

Appendix

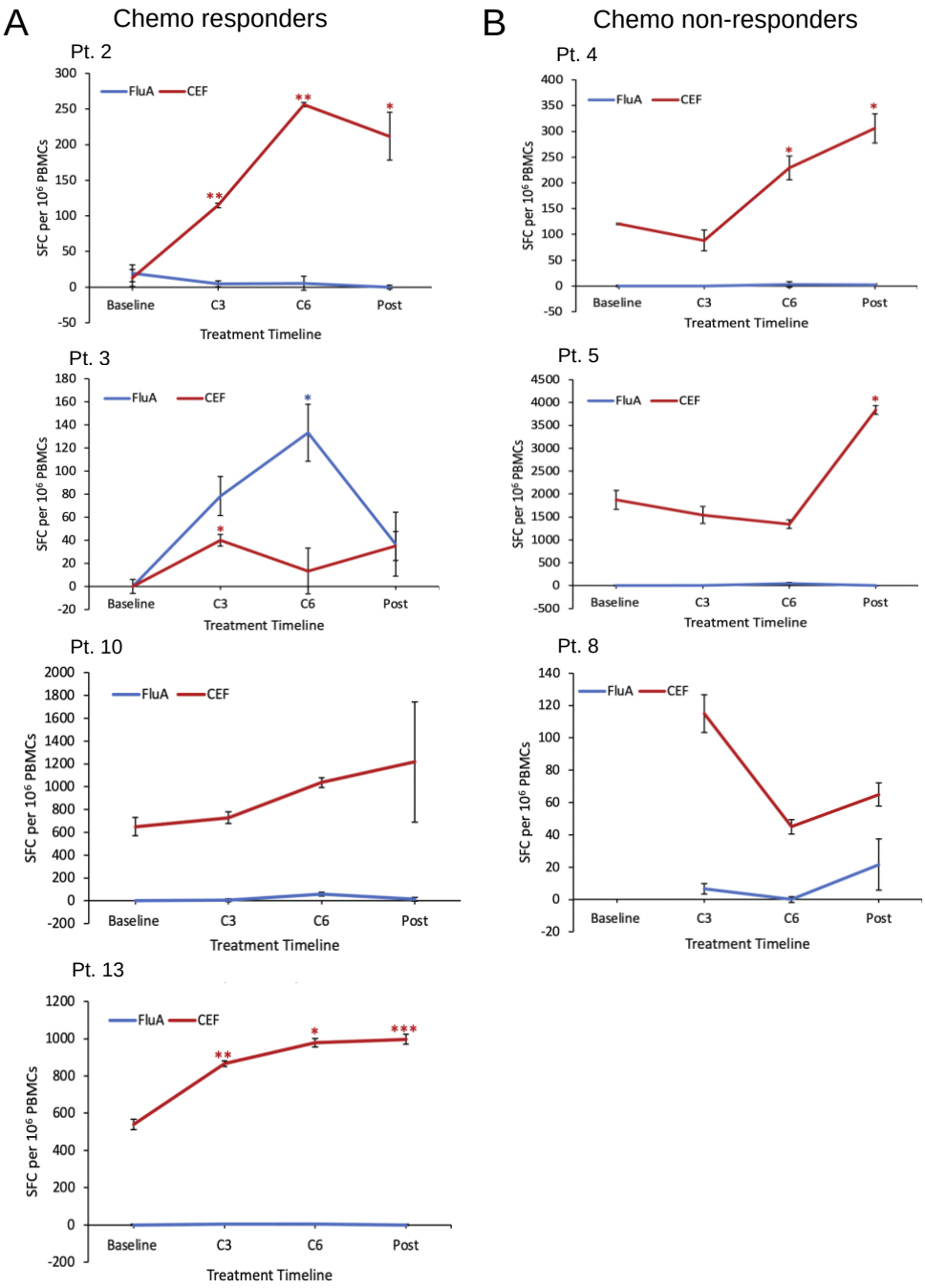

Extended Data Figure 1. Circulating T cell responses to viral antigens throughout chemotherapy in chemo responders and chemo non-responders

(A, B) IFNγ ELISPOT responses for PBMCs over the course of chemotherapy. ELISPOT data were background (OVA)-subtracted with n = 3 biologically independent samples. Each data was mean ± standard error of the mean (s.e.m.). Repeated-measures regression model with Dunnett's multiple comparison test was used for generating p values. $*P \leq 0.5$ $**P \leq 0.05$ $***P \leq 0.005$.

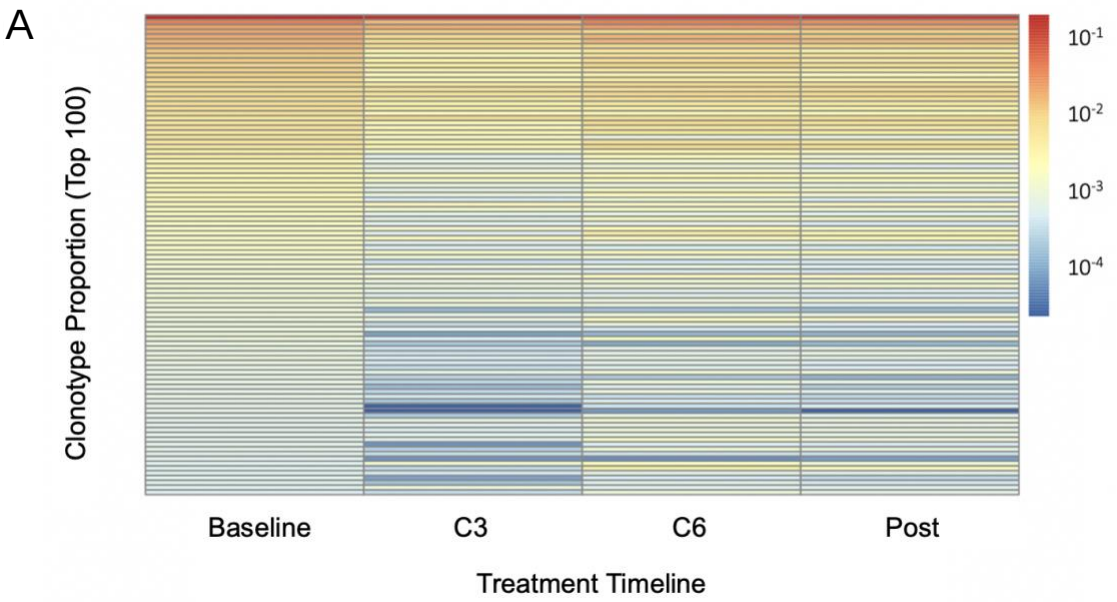

Extended Data Figure 2. TCR repertoire dynamics across timepoints of chemotherapy
(A) Proportions of top 100 clonotypes over the course of chemotherapy treatment in patient 2. Top 100 clonotypes were ranked according to the clonotype proportion of Baseline. Total clonotypes at Baseline, C3, C6, and Post were 17040, 22351, 51254, and 41719 respectively.

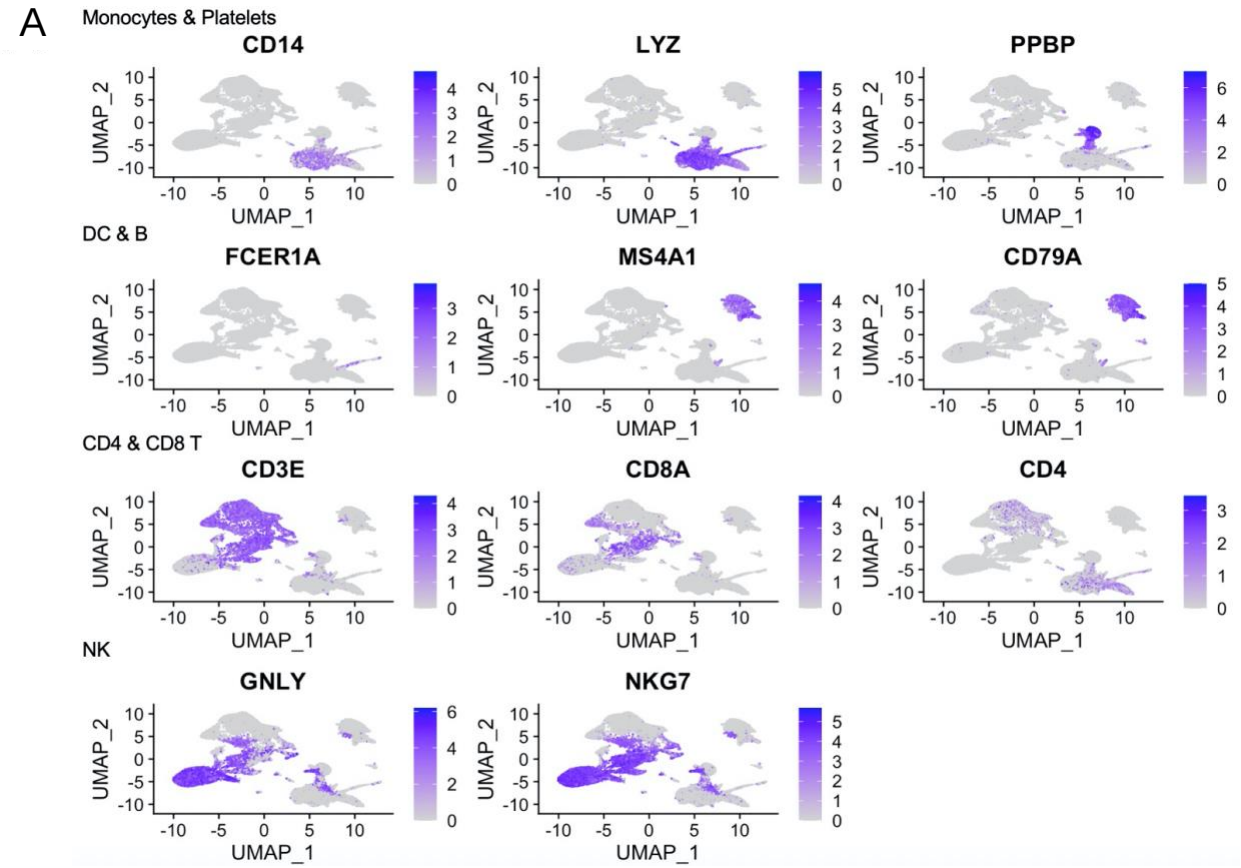

Extended Data Figure 3. Transcriptional profile of integrated PBMCs for cell type identification

(A) Feature plots of selected marker genes for the integrated clusters of patients 2, 3, 4, 9, and 13.

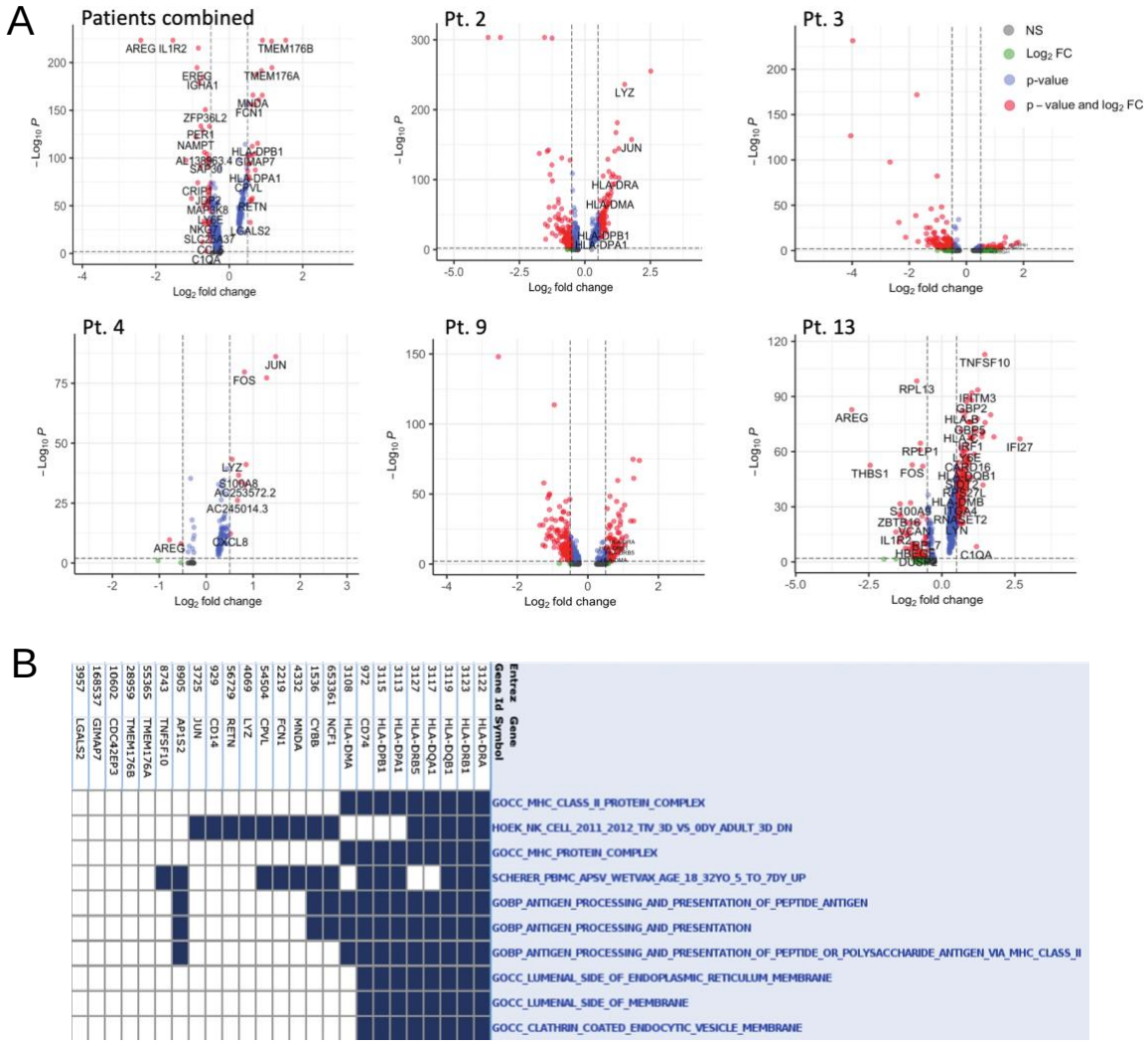

Extended Data Figure 4. Differential expression analysis of the transcriptional changes in monocyte population before and after chemotherapy

(A) Differentially expressed gene expression in the combined and individual datasets of patients 2, 3, 4, 9, and 13. Blue dots represented differentially expressed genes with false discovery rate-corrected P value < 0.01. Green dots represented differentially expressed genes with log2 fold change > 0.5. Red dots represented genes with false discovery rate-corrected P value < 0.01 and log2 fold change > 0.5. Positive values indicated the upregulated genes after the third cycle of chemotherapy. **(B)** Gene set enrichment analysis of all the upregulated genes in the monocyte population after chemotherapy for all patients.

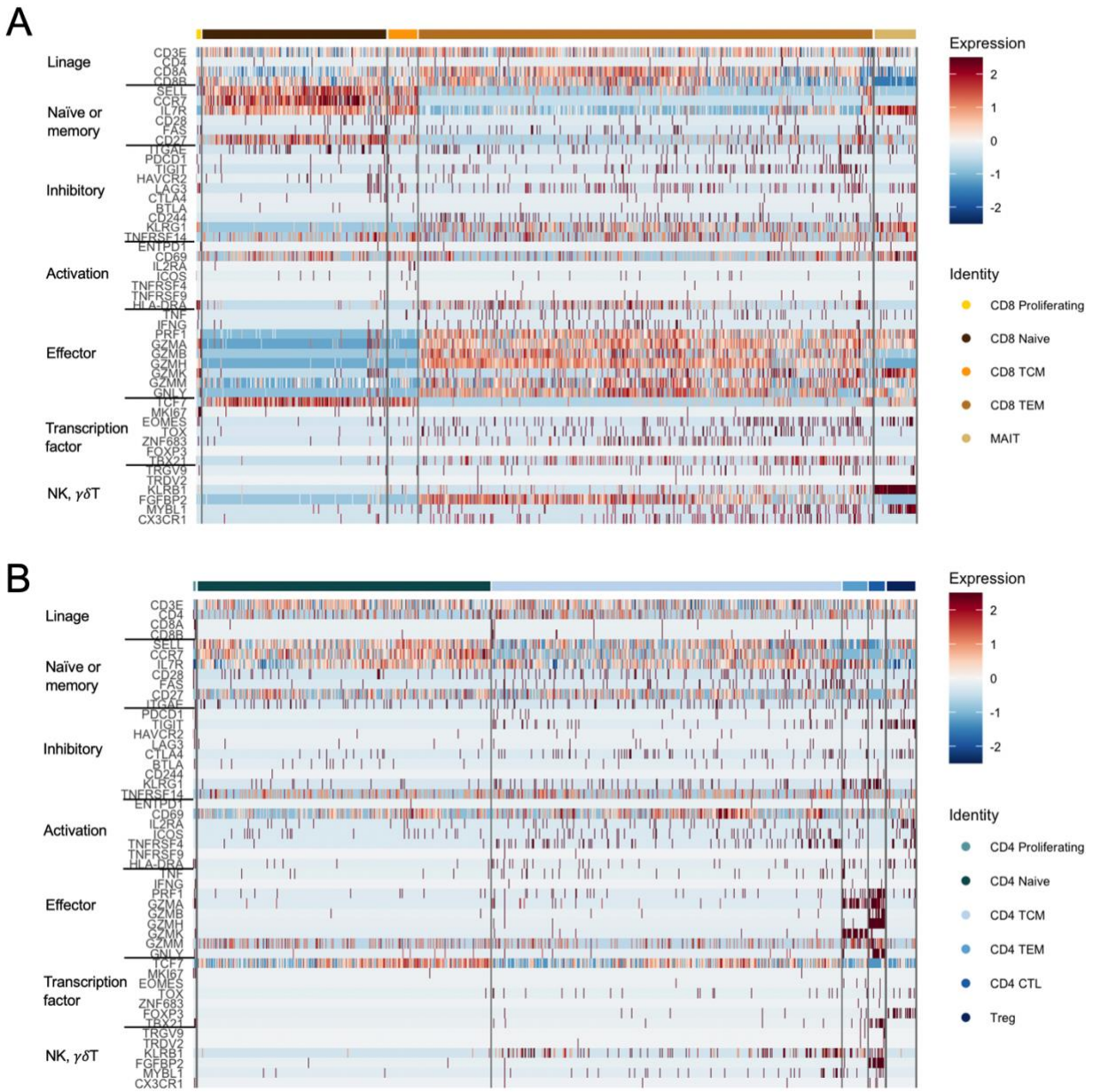

Extended Data Figure 5. Transcriptional profile of CD8$^+$ and CD4$^+$ T cells by cluster
(A, B) Heat map of gene expressions based on markers in the categories of linage, naïve or memory, inhibitory, activation, effector, transcription factor, and NK/γδ T signatures by cluster of CD8$^+$ (A) and CD4$^+$ (B) T cells.

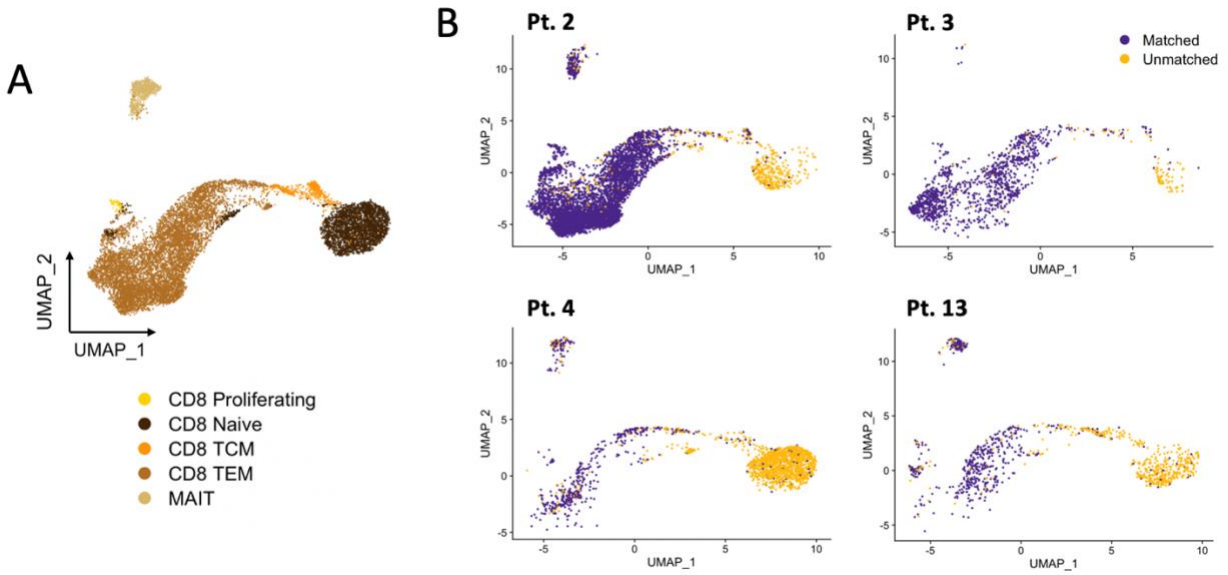

Extended Data Figure 6. Matched CD8$^+$ T cell clonotypes between single-cell and bulk TCR sequencing

(A) UMAP of the CD8$^+$ T cells subclusters. **(B)** UMAP of the matched and unmatched CD8$^+$ T cell clonotypes between single cell and bulk TCR sequencing in patient 2, 3, 4, and 13. CD8$^+$ T cell clonotypes of single cell and bulk TCR sequencing were matched by CDR3 amino acid of TCR beta chain.

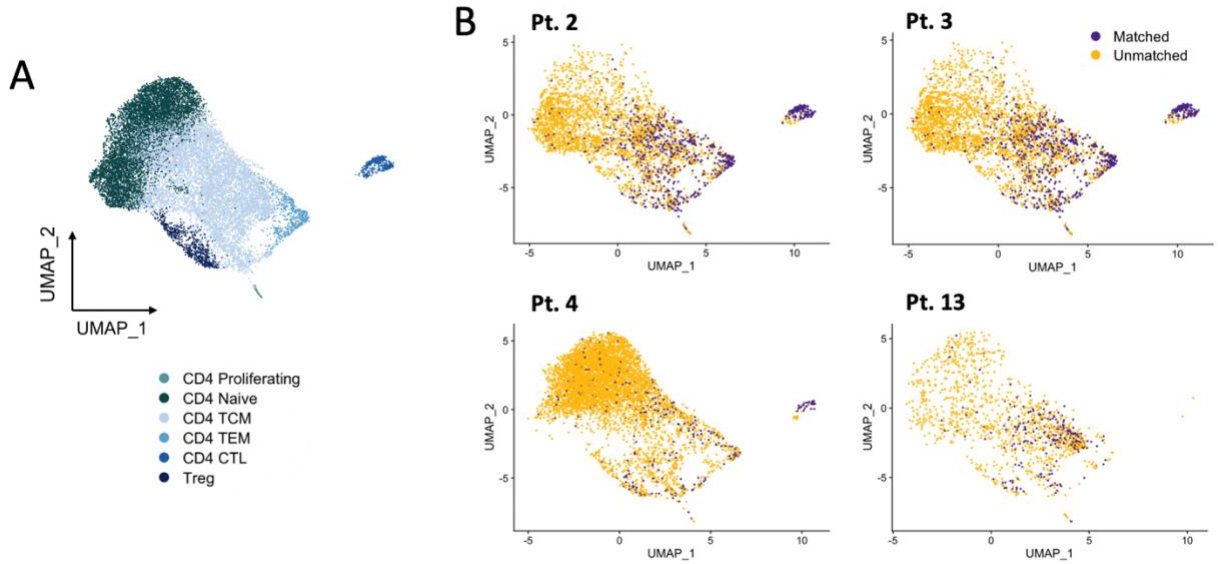

Extended Data Figure 7. Matched CD4$^+$ T cell clonotypes between single-cell and bulk TCR sequencing

(A) UMAP of the CD4$^+$ T cells subclusters. **(B)** UMAP of the matched and unmatched CD4$^+$ T cell clonotypes between single cell and bulk TCR sequencing in patient 2, 3, 4, and 13. CD4$^+$ T cell clonotypes of single cell and bulk TCR sequencing were matched by CDR3 amino acid of TCR beta chain.